Neutrino Cross Sections with NOvA

Kevin Vockerodt
on behalf of the NOvA Collaboration

35th Rencontres de Blois
Thursday 24th October 2024

The NOvA Experiment

- Long baseline neutrino experiment, consisting of:
  - NuMI beam: high purity (anti)neutrino beam produced at Fermilab
  - Forward horn current (FHC) mode for a muon neutrino (ν_μ) beam
  - Reverse horn current (RHC) mode for a muon antineutrino ($\bar{\nu}_\mu$) beam
  - Near Detector: 1km from the source, 100m underground
  - Far Detector: 810km from the source in Ash River, Minnesota, at ground level

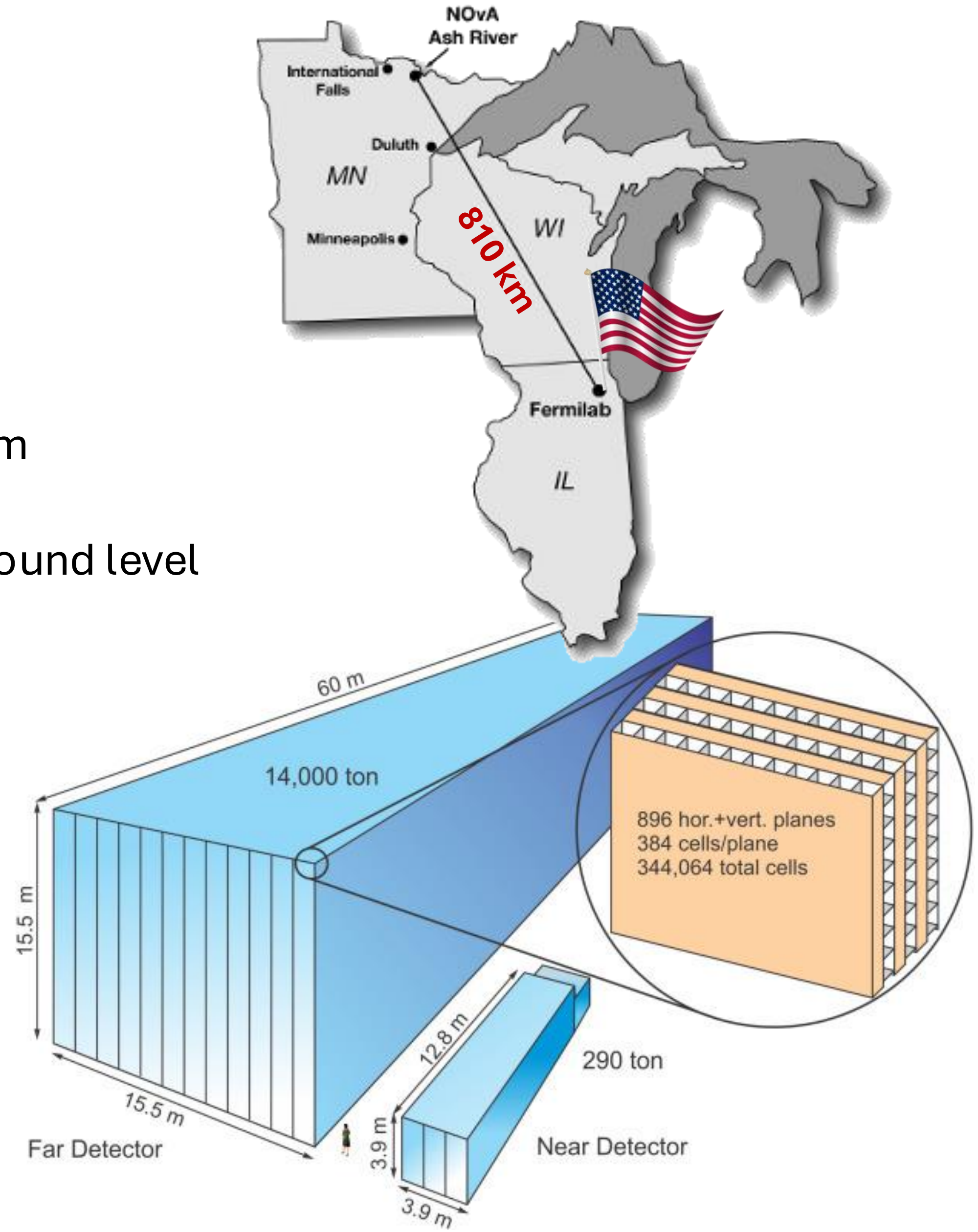

The NOvA Experiment

- Long baseline neutrino experiment, consisting of:
  - NuMI beam: high purity (anti)neutrino beam produced at Fermilab
  - Forward horn current (FHC) mode for a muon neutrino (ν_μ) beam
  - Reverse horn current (RHC) mode for a muon antineutrino ($\bar{\nu}_\mu$) beam
  - Near Detector: 1km from the source, 100m underground
  - Far Detector: 810km from the source in Ash River, Minnesota, at ground level

- Detectors are 14.6 mrad off-axis and functionally identical, helping to reduce systematic uncertainties

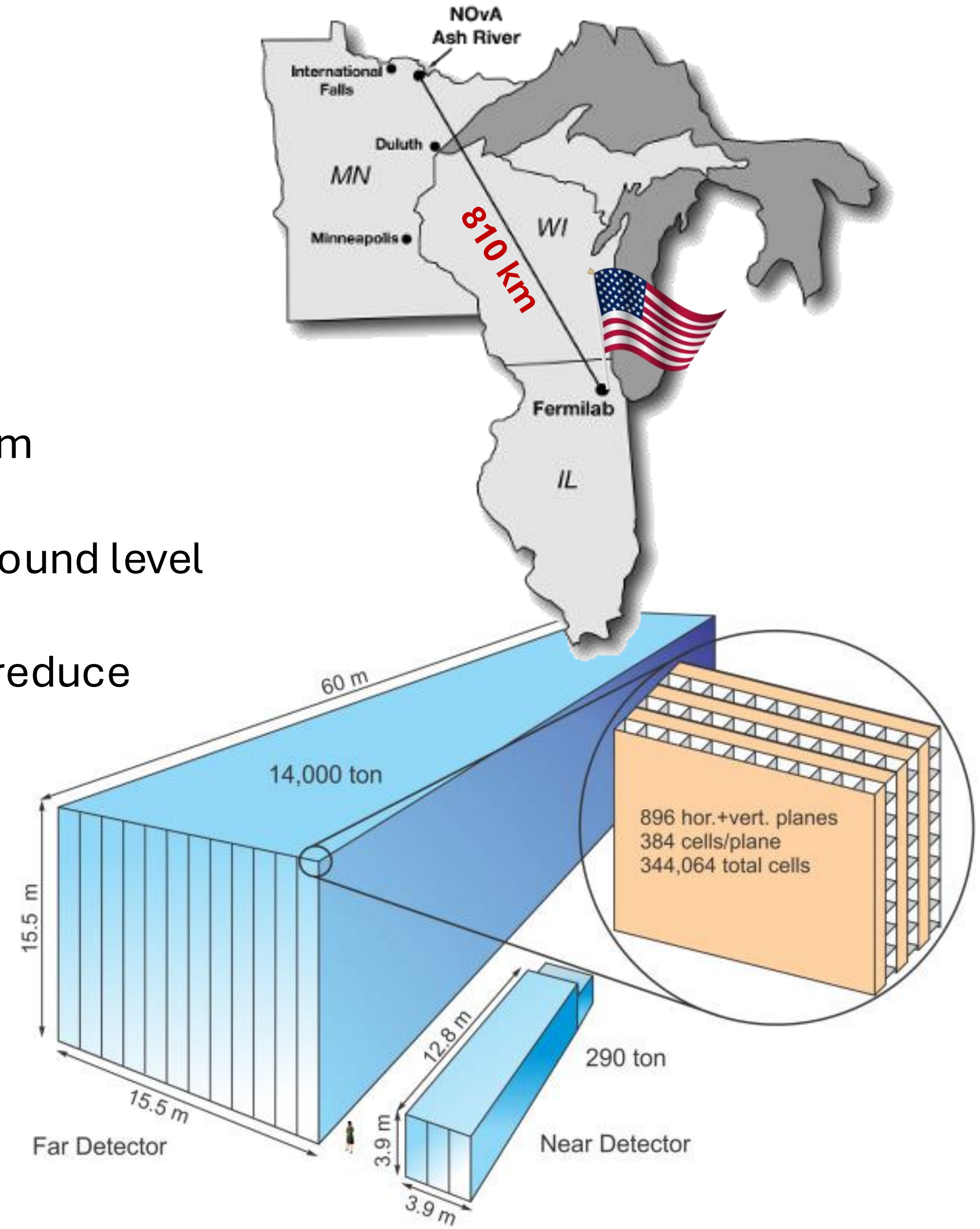

The NOvA Experiment

- Long baseline neutrino experiment, consisting of:
  - NuMI beam: high purity (anti)neutrino beam produced at Fermilab
  - Forward horn current (FHC) mode for a muon neutrino (ν_μ) beam
  - Reverse horn current (RHC) mode for a muon antineutrino ($\overline{\nu}_\mu$) beam
  - Near Detector: 1km from the source, 100m underground
  - Far Detector: 810km from the source in Ash River, Minnesota, at ground level
- Detectors are 14.6 mrad off-axis and functionally identical, helping to reduce systematic uncertainties
- Three research goals:
  - Observe and measure oscillation of ν_μ to ν_e
  - Determine neutrino mass ordering
  - Investigate matter / antimatter asymmetry

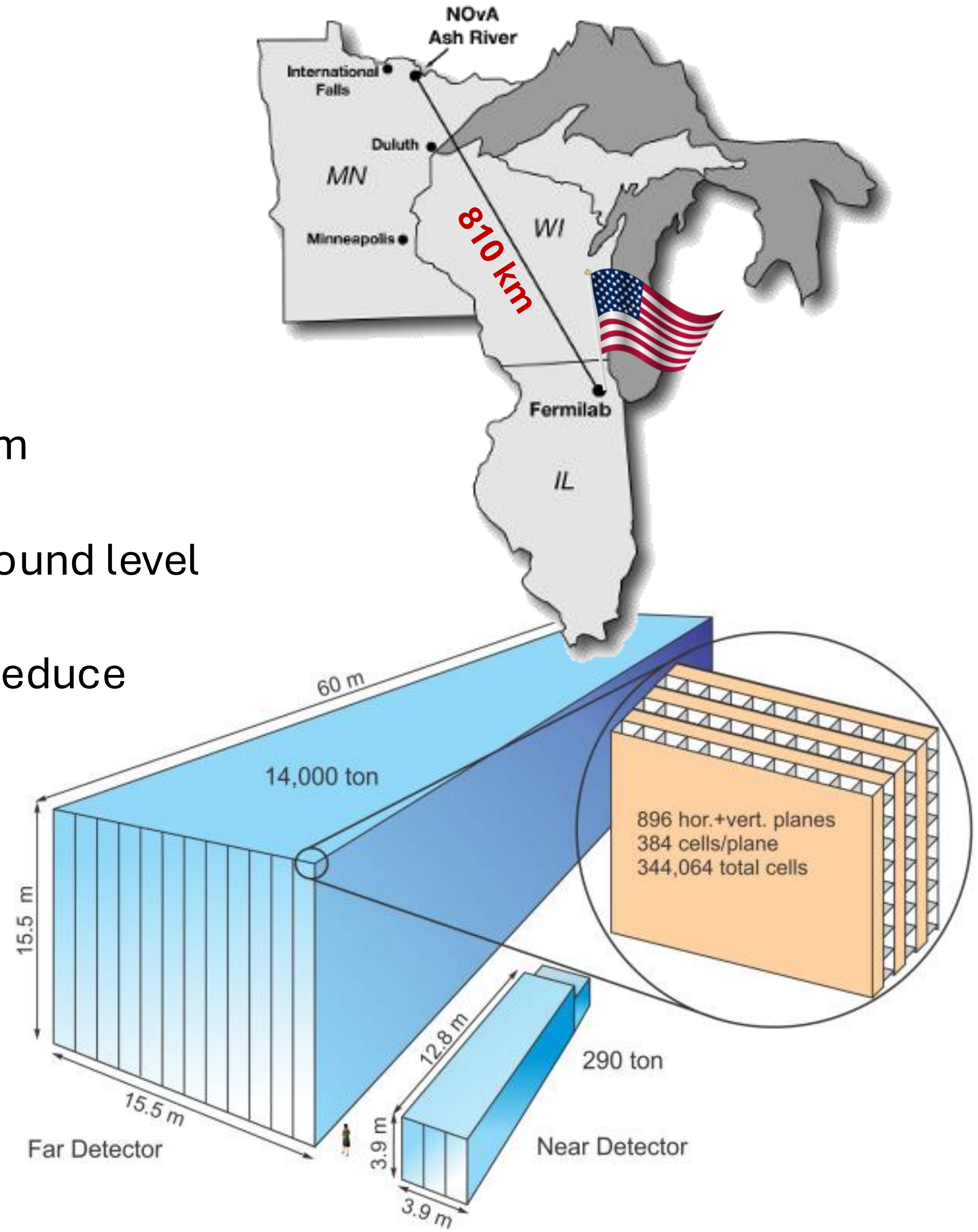

The NOvA Near Detector

- 300t tracking calorimeter
- Extruded plastic (PVC) cells filled with liquid scintillator
- Alternating planes allow for 3D reconstruction

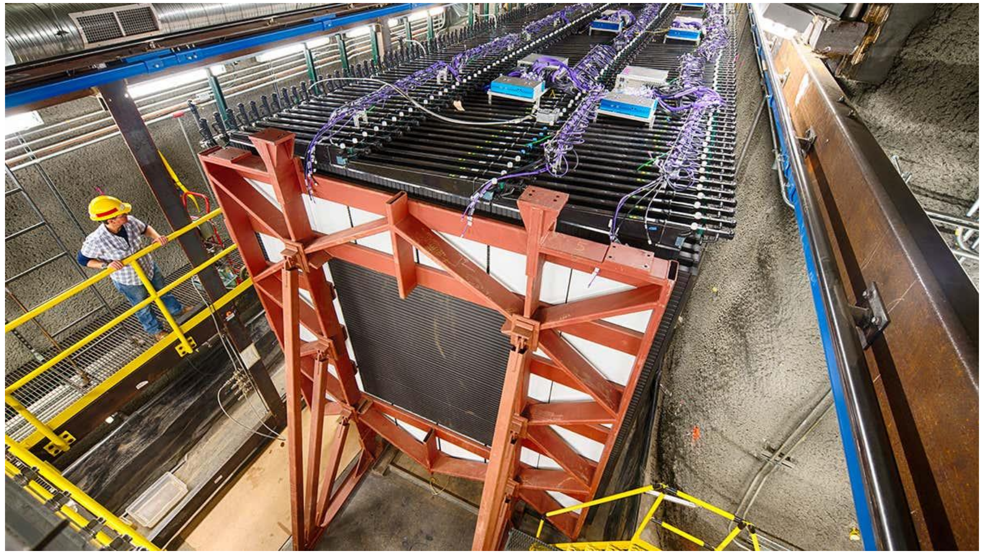

The NOvA Near Detector

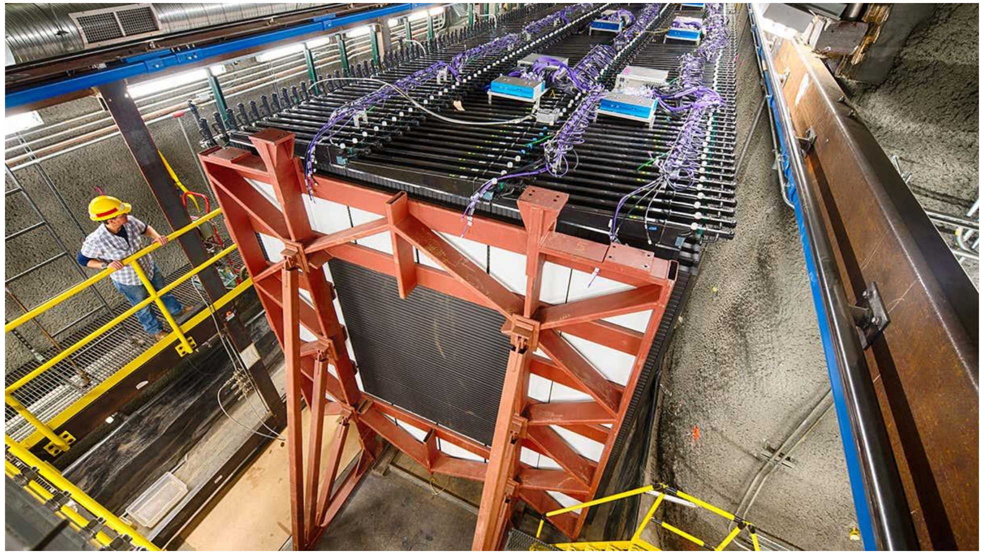

- 300t tracking calorimeter
- Extruded plastic (PVC) cells filled with liquid scintillator
- Alternating planes allow for 3D reconstruction

NOvA Detector Composition (by mass)				
H	C	Cl	O	Ti
11%	67%	16%	3%	3%

The NOvA Near Detector

- 300t tracking calorimeter
- Extruded plastic (PVC) cells filled with liquid scintillator
- Alternating planes allow for 3D reconstruction

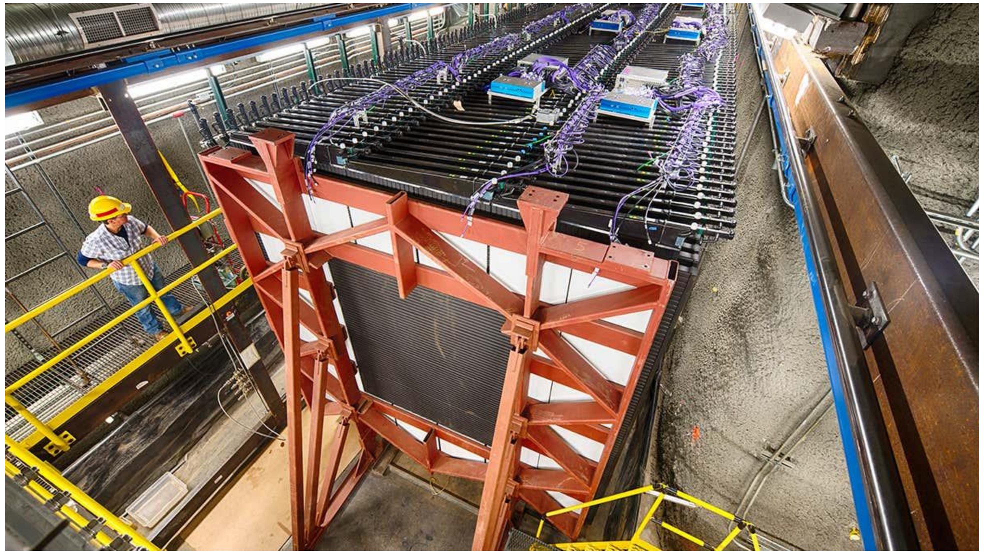

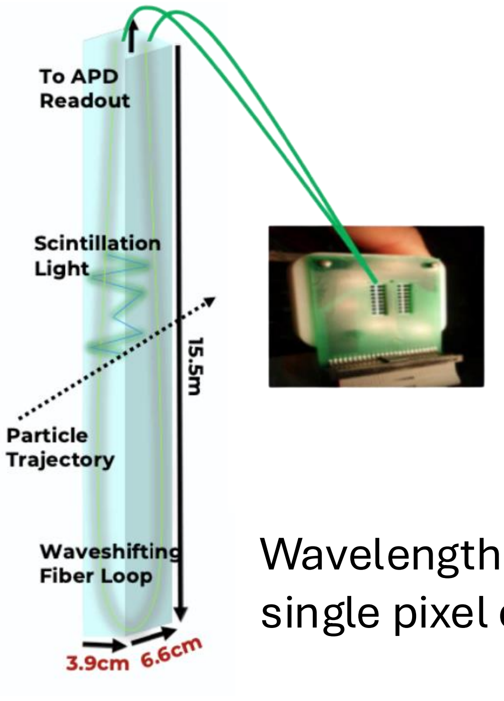

NOvA Detector Composition (by mass)				
H	C	Cl	O	Ti
11%	67%	16%	3%	3%

Wavelength shifting fibres are read out by a single pixel on Avalanche Photodiode (APD)

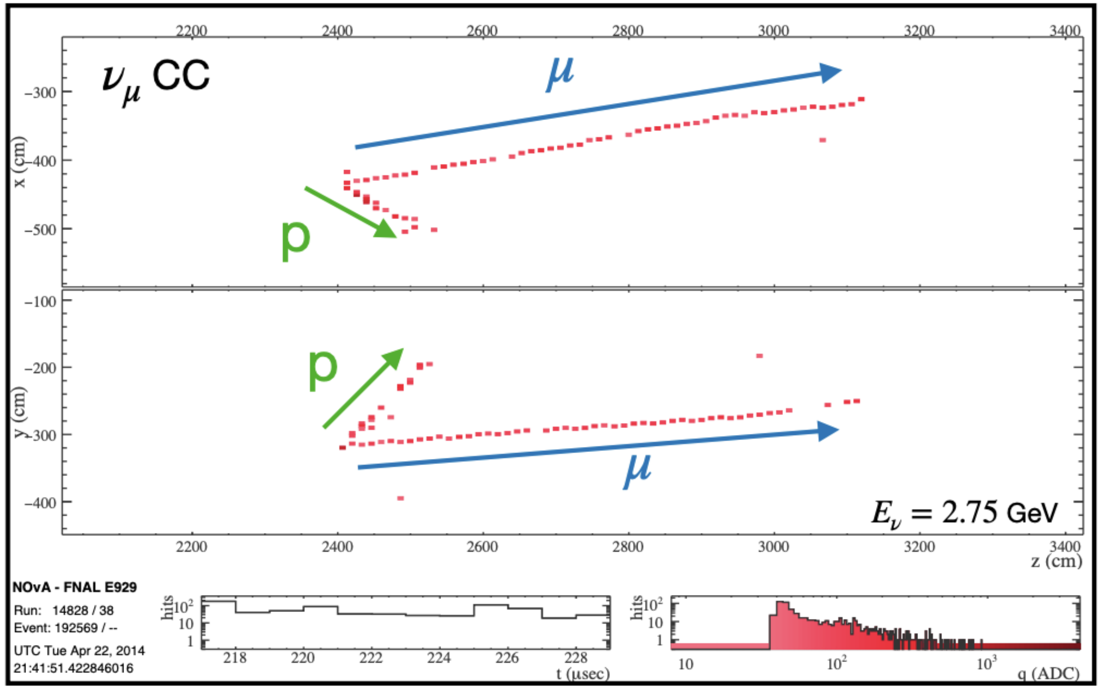

Why are Cross Sections Important in Oscillation Analyses?

To understand neutrino oscillations, we need to make precision measurements of the neutrino mixing angles (e.g. θ_{23} and θ_{13}) and mass splittings (e.g. Δm^2_{32}).

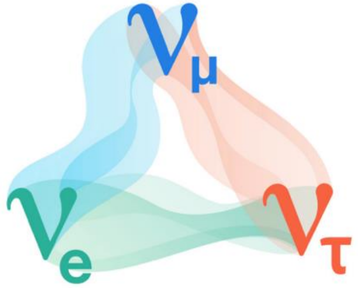

Why are Cross Sections Important in Oscillation Analyses?

To understand neutrino oscillations, we need to make precision measurements of the neutrino mixing angles (e.g. θ_{23} and θ_{13}) and mass splittings (e.g. Δm^2_{32}).

Oscillation probability (electron neutrino appearance)

$$P(\nu_\mu \rightarrow \nu_e) \simeq \sin^2 \theta_{23} \sin^2 2\theta_{13} \sin^2 \frac{1.27 \, \Delta m^2_{32} \, L \, [\text{km}]}{E \, [\text{GeV}]}$$

L Distance between detectors

E Mean neutrino beam energy

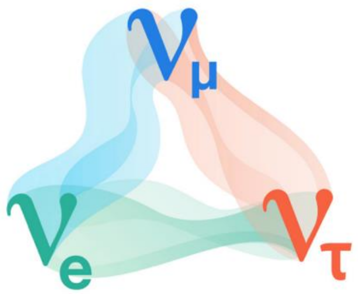

Why are Cross Sections Important in Oscillation Analyses?

To understand neutrino oscillations, we need to make precision measurements of the neutrino mixing angles (e.g. θ_{23} and θ_{13}) and mass splittings (e.g. Δm^2_{32}).

Oscillation probability (electron neutrino appearance)

$$P(\nu_\mu \rightarrow \nu_e) \simeq \sin^2 \theta_{23} \sin^2 2\theta_{13} \sin^2 \frac{1.27\, \Delta m^2_{32}\, L\,[\mathrm{km}]}{E\,[\mathrm{GeV}]}$$

L Distance between detectors

E Mean neutrino beam energy

Measured event rate

$$R(\vec{x}) = \int_{E_{\min}}^{E_{\max}} \Phi(E_\nu) \times \sigma(E_\nu, \vec{x}) \times \epsilon(\vec{x}) \times P(\nu_\mu \rightarrow \nu_e)$$

$\Phi(E_\nu)$ Neutrino flux

$\sigma(E_\nu, \vec{x})$ Cross section

$\epsilon(\vec{x})$ Detector response / efficiency

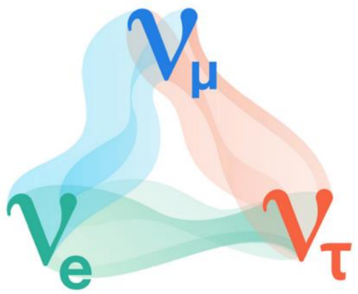

Cross Section Uncertainties

- Until recently, neutrino experiments have been statistically-limited, with a statistical uncertainty ~10 – 25%
- But next-generation experiments, e.g. DUNE and Hyper-K expect to observe up to two orders of magnitude more events, reducing statistical uncertainties to ~3% for ν_e and ~1% for ν_μ
- We are therefore entering an era where uncertainties are systematics-dominant, so we need better constraints

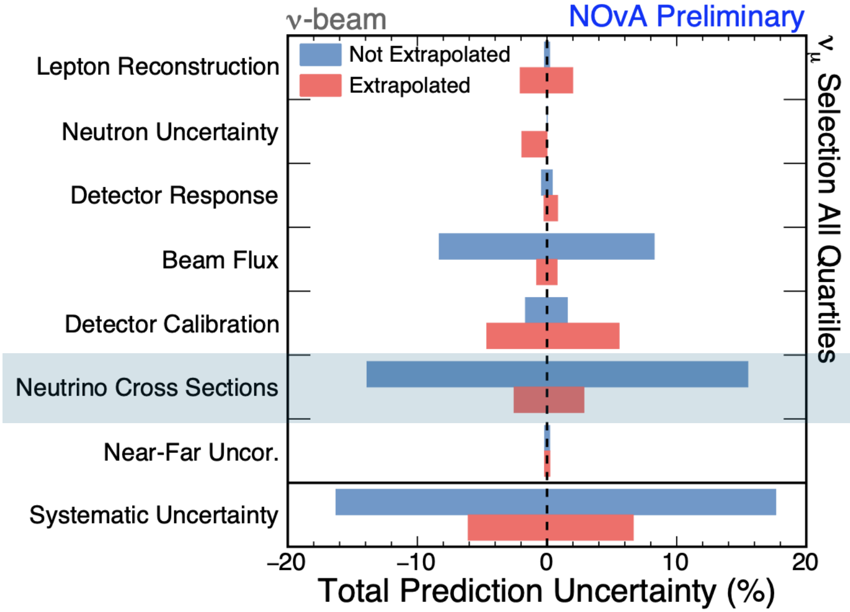

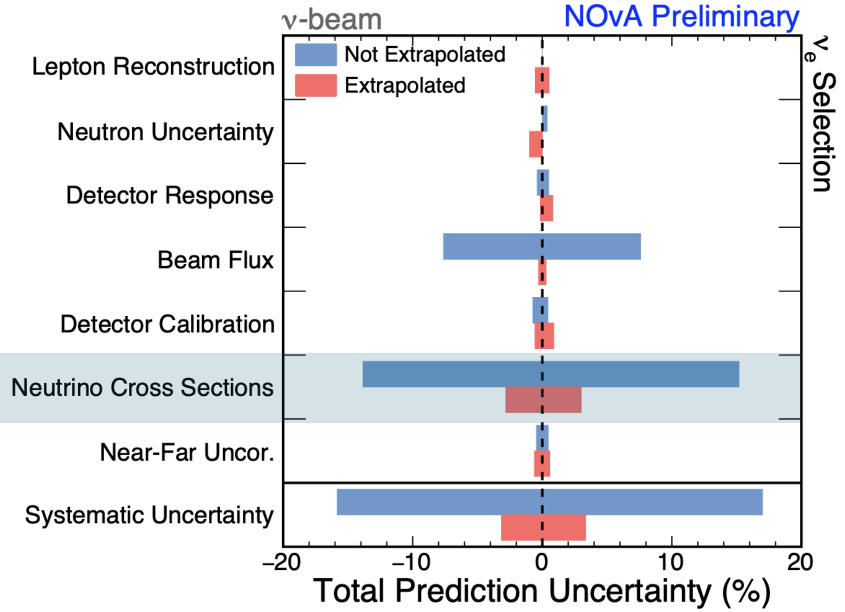

Neutrino Interactions and Nuclear Effects

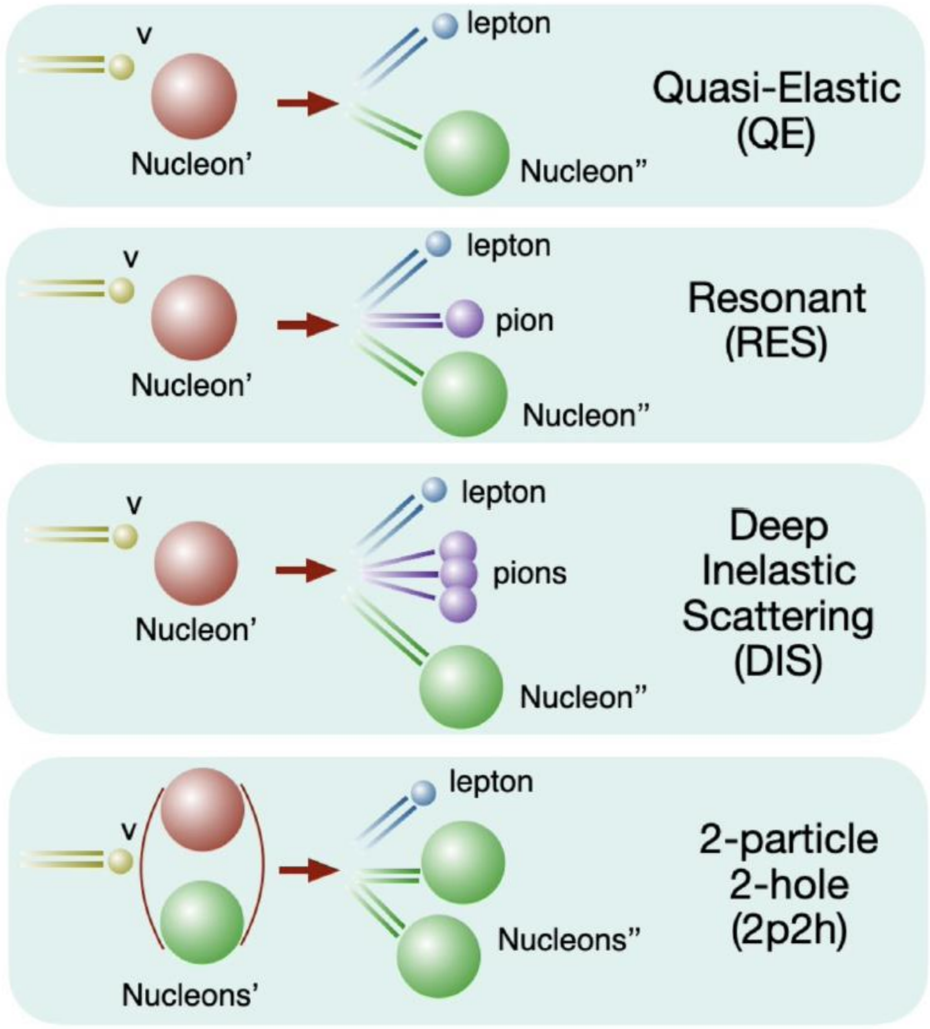

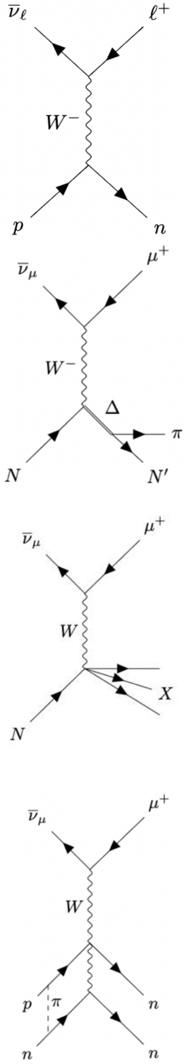

Credit: L. Cremonesi (Neutrino 2020)

The Meson Exchange Current (MEC) model is the leading 2p2h model.

J. Formaggio and G. Zeller (arxiv:1305.7513) *(adapted)*

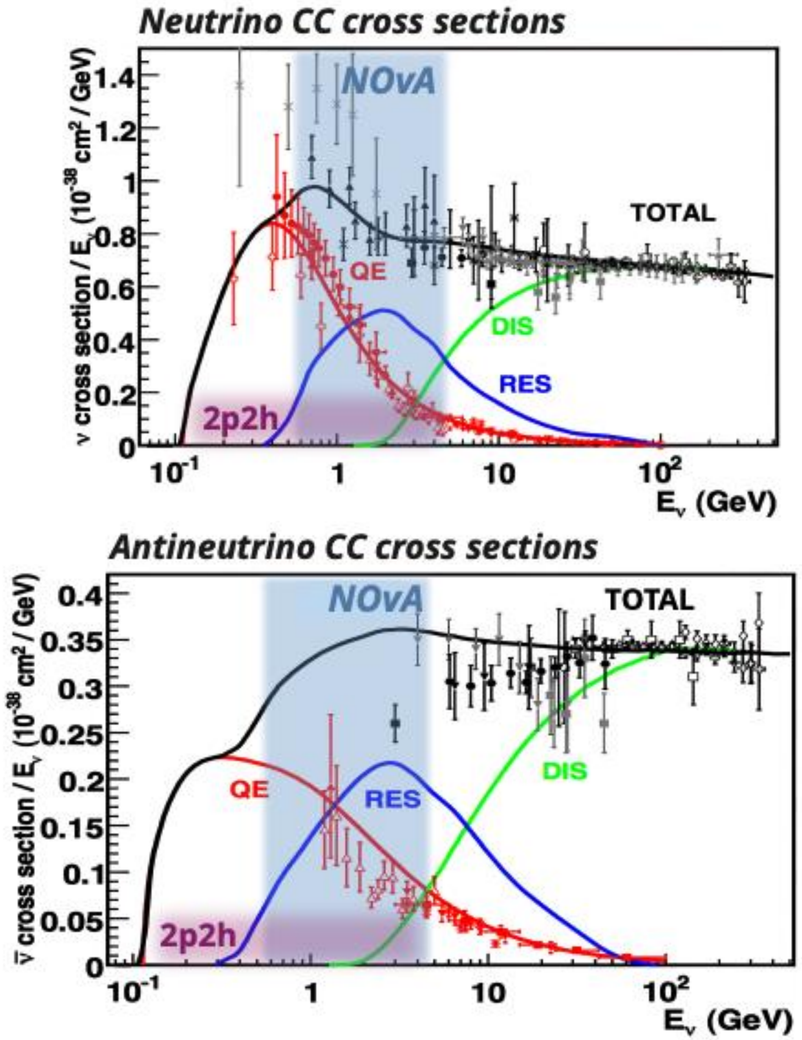

Neutrino Interactions and Nuclear Effects

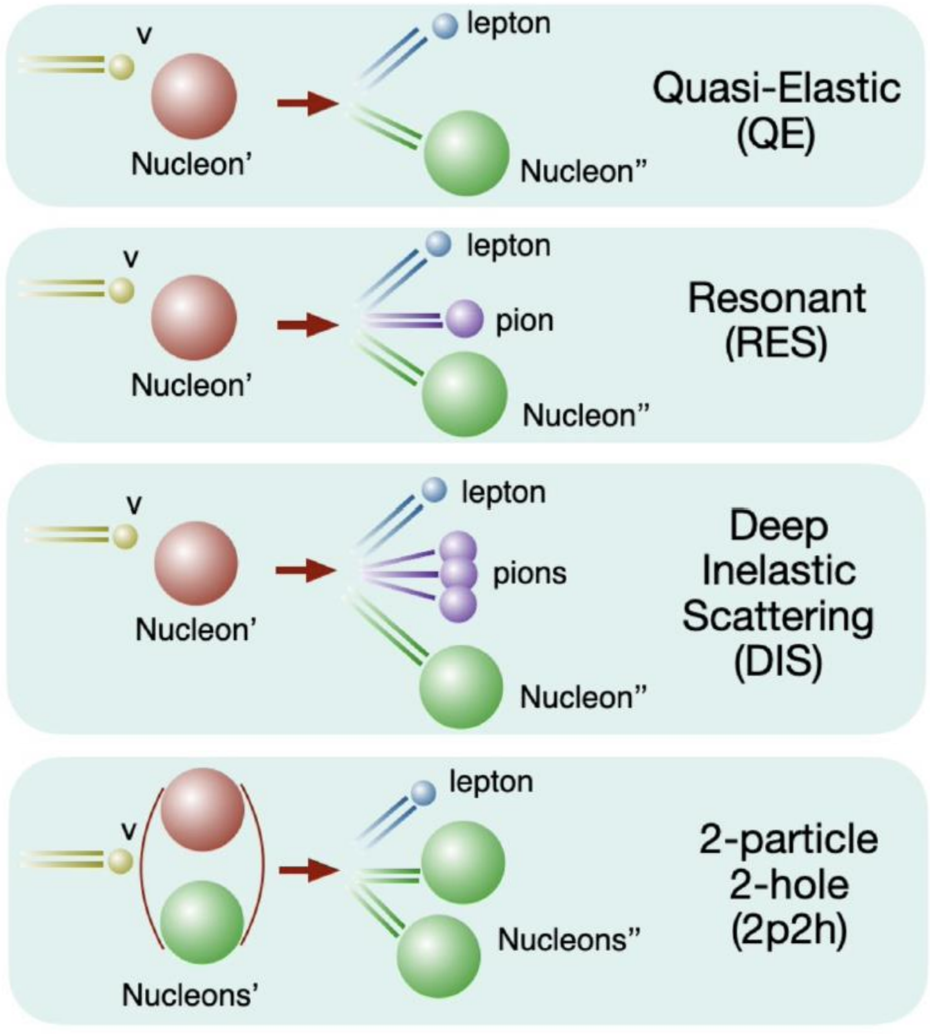

Credit: L. Cremonesi (Neutrino 2020)

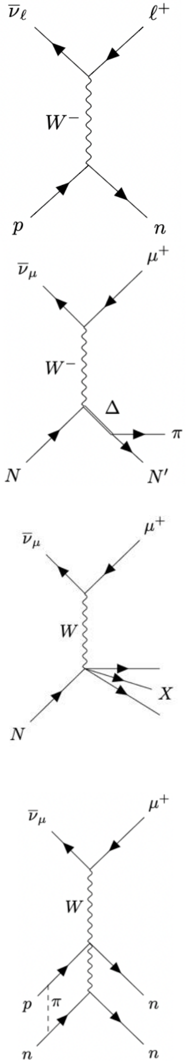

The Meson Exchange Current (MEC) model is the leading 2p2h model.

Final State Interactions (FSI) can alter the particle output and kinematics

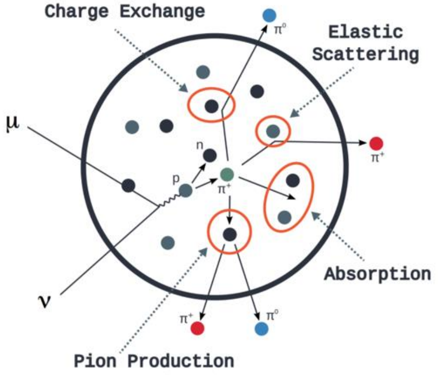

Credit: T. Golan

J. Formaggio and G. Zeller (arxiv:1305.7513) *(adapted)*

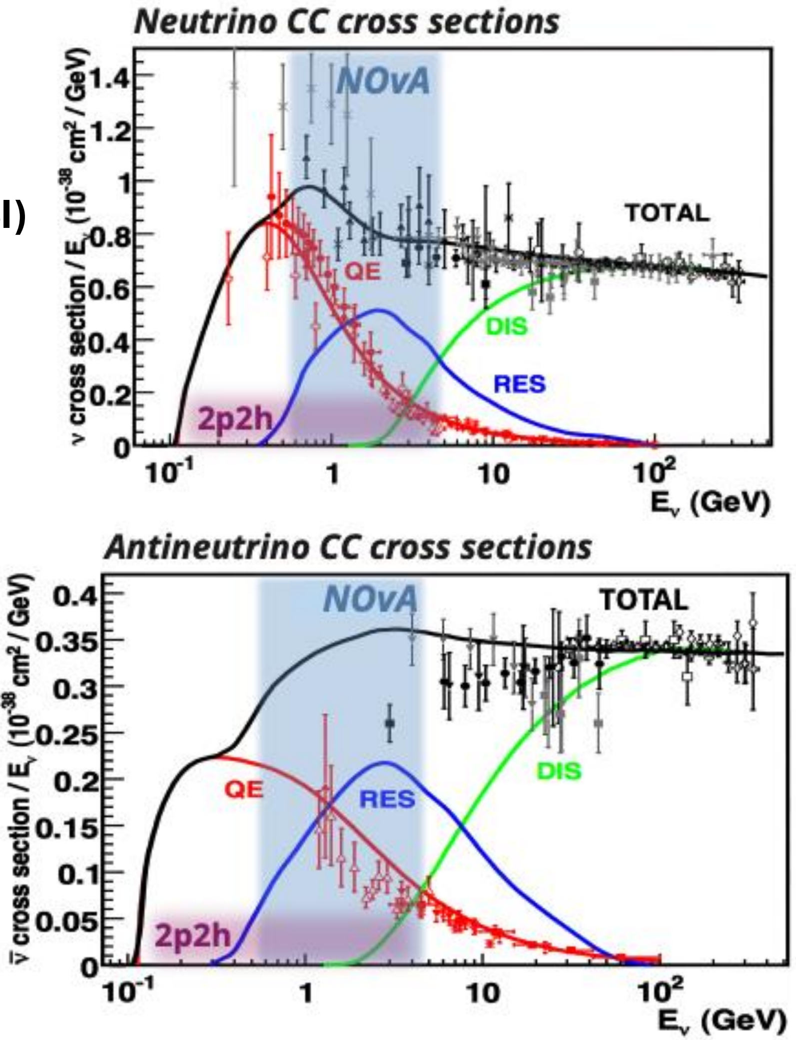

The NOvA Simulation

- The most recent NOvA simulation uses GENIE 3.0.6 as its base model, but some some analyses shown today use GENIE v2
- MEC and FSI are adjusted to data to produce a NOvA-specific tuned interaction model
- This tuning is performed in variables that are different to this analysis
- The MEC tune was developed using neutrino data and then applied to antineutrinos

GENIE version	Initial State	QE	MEC	RES/COH	DIS	FSI
2.10.2 / 2.12.2	Relativistic Fermi Gas (RFG)	Llewellyn-Smith	Empirical	Rein-Sehgal (RS)	Bodek-Yang + Pythia	hA (one effective interaction)
3.0.6	Local Fermi Gas (LFG)	València + Z-expansion	València	Berger-Sehgal (BS)	Bodek-Yang + Pythia	hN (semi-classical cascade model – many possible interactions)

$\overline{\nu}_\mu$ CC-inclusive Cross Section Analysis

(Paper currently in preparation)

GENIE 3.0.6

- **Signal:** $\overline{\nu}_\mu$ CC interaction with interaction vertex in the fiducial volume of the ND
- $\overline{\nu}_\mu + A \to \mu^+ + X$
- A is the target nucleus, X represents all other final state particles

- **Deliverables:**
  - Triple differential cross section in T_μ, $\cos\theta_\mu$ and E_{avail}
  - 1D measurement of E_ν and Q^2

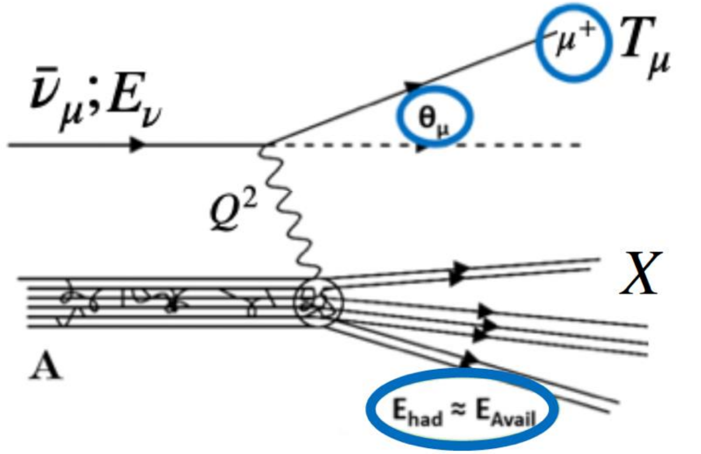

Credit: Travis Olson

$\bar{\nu}_\mu$ CC-inclusive Cross Section Analysis

(Paper currently in preparation)

GENIE 3.0.6

- **Signal:** $\bar{\nu}_\mu$ CC interaction with interaction vertex in the fiducial volume of the ND
- $\bar{\nu}_\mu + A \rightarrow \mu^+ + X$
- A is the target nucleus, X represents all other final state particles

- **Deliverables:**
  - Triple differential cross section in T_μ, $\cos\theta_\mu$ and E_{avail}
  - 1D measurement of E_ν and Q^2

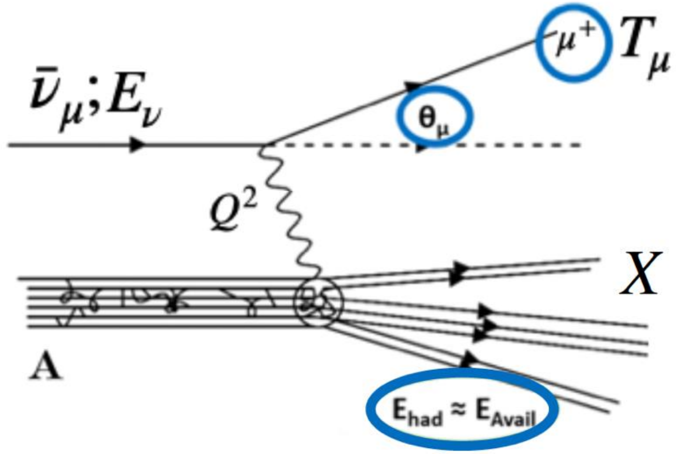

Credit: Travis Olson

- **E_{avail}:**
  - Variable introduced by the MINERvA collaboration: Phys. Rev. Lett. 116, 071802 (2016)
  - It comprises of the total visible hadronic energy
  - Neutrons are not directly visible and do not contribute to E_{avail}, but any daughter particles of primary neutrons do contribute
  - Different regions of E_{avail} phase space enhance different interaction types

$\bar{\nu}_\mu$ CC-inclusive: Triple Differential Cross Section Measurement Strategy

$$\left(\frac{d^3\sigma}{d\cos\theta_\mu\, dT_\mu\, dE_{avail}}\right)_i = \frac{\sum_j U_{ij}\left(N^{\text{sel}}\left(\cos\theta_\mu, T_\mu, E_{avail}\right)_j P\left(\cos\theta_\mu, T_\mu, E_{avail}\right)_j \right)}{\epsilon\left(\cos\theta_\mu, T_\mu, E_{avail}\right)_i \left(\Delta\cos\theta_\mu\right)_i \left(\Delta T_\mu\right)_i \left(\Delta E_{avail}\right)_i N_{\text{targets}}\, \Phi}$$

i truth space
j reco space

$\bar{\nu}_\mu$ CC-inclusive: Triple Differential Cross Section Measurement Strategy

$$\left(\frac{d^3\sigma}{d\cos\theta_\mu \, dT_\mu \, dE_{avail}}\right)_i = \frac{\sum_j U_{ij} \left(N^{\mathrm{sel}}\left(\cos\theta_\mu, T_\mu, E_{avail}\right)_j P\left(\cos\theta_\mu, T_\mu, E_{avail}\right)_j \right)}{\epsilon\left(\cos\theta_\mu, T_\mu, E_{avail}\right)_i \left(\Delta\cos\theta_\mu\right)_i \left(\Delta T_\mu\right)_i \left(\Delta E_{avail}\right)_i \, N_{\mathrm{targets}} \, \Phi}$$

i truth space

j reco space

$N^{\mathrm{sel}}\left(\cos\theta_\mu, T_\mu, E_{avail}\right)_j$ Number of selected events

$\bar{\nu}_\mu$ CC-inclusive: Triple Differential Cross Section Measurement Strategy

$$\left(\frac{d^3\sigma}{d\cos\theta_\mu\, dT_\mu\, dE_{avail}}\right)_i = \frac{\sum_j U_{ij}\left(N^{\text{sel}}\left(\cos\theta_\mu, T_\mu, E_{avail}\right)_j P\left(\cos\theta_\mu, T_\mu, E_{avail}\right)_j \right)}{\epsilon\left(\cos\theta_\mu, T_\mu, E_{avail}\right)_i \left(\Delta\cos\theta_\mu\right)_i \left(\Delta T_\mu\right)_i \left(\Delta E_{avail}\right)_i N_{\text{targets}}\, \Phi}$$

i truth space
j reco space

$N^{\text{sel}}\left(\cos\theta_\mu, T_\mu, E_{avail}\right)_j$ Number of selected events

$P\left(\cos\theta_\mu, T_\mu, E_{avail}\right)_j$ Purity of sample (estimated from simulation)

$\bar{\nu}_\mu$ CC-inclusive: Triple Differential Cross Section Measurement Strategy

$$\left(\frac{d^3\sigma}{d\cos\theta_\mu\, dT_\mu\, dE_{avail}}\right)_i = \frac{\sum_j U_{ij}\left(N^{\mathrm{sel}}\left(\cos\theta_\mu, T_\mu, E_{avail}\right)_j P\left(\cos\theta_\mu, T_\mu, E_{avail}\right)_j \right)}{\epsilon\left(\cos\theta_\mu, T_\mu, E_{avail}\right)_i \left(\Delta\cos\theta_\mu\right)_i \left(\Delta T_\mu\right)_i \left(\Delta E_{avail}\right)_i N_{\mathrm{targets}}\, \Phi}$$

i truth space

j reco space

$N^{\mathrm{sel}}\left(\cos\theta_\mu, T_\mu, E_{avail}\right)_j$ Number of selected events

$P\left(\cos\theta_\mu, T_\mu, E_{avail}\right)_j$ Purity of sample (estimated from simulation)

U_{ij} Unfolding Matrix – to migrate from reco to truth space, using D'Agostini iterative unfolding

$\bar{\nu}_\mu$ CC-inclusive: Triple Differential Cross Section Measurement Strategy

$$\left(\frac{d^3\sigma}{d\cos\theta_\mu\, dT_\mu\, dE_{avail}}\right)_i = \frac{\sum_j U_{ij}\left(N^{\text{sel}}\left(\cos\theta_\mu, T_\mu, E_{avail}\right)_j P\left(\cos\theta_\mu, T_\mu, E_{avail}\right)_j \right)}{\epsilon\left(\cos\theta_\mu, T_\mu, E_{avail}\right)_i \left(\Delta\cos\theta_\mu\right)_i \left(\Delta T_\mu\right)_i \left(\Delta E_{avail}\right)_i N_{\text{targets}}\, \Phi}$$

i truth space

j reco space

$N^{\text{sel}}\left(\cos\theta_\mu, T_\mu, E_{avail}\right)_j$ Number of selected events

$P\left(\cos\theta_\mu, T_\mu, E_{avail}\right)_j$ Purity of sample (estimated from simulation)

U_{ij} Unfolding Matrix – to migrate from reco to truth space, using D'Agostini iterative unfolding

$\epsilon\left(\cos\theta_\mu, T_\mu, E_{avail}\right)_i$ Efficiency of sample (estimated from simulation)

$\bar{\nu}_\mu$ CC-inclusive: Triple Differential Cross Section Measurement Strategy

$$\left(\frac{d^3\sigma}{d\cos\theta_\mu\, dT_\mu\, dE_{avail}}\right)_i = \frac{\sum_j U_{ij}\left(N^{\text{sel}}\left(\cos\theta_\mu, T_\mu, E_{avail}\right)_j P\left(\cos\theta_\mu, T_\mu, E_{avail}\right)_j \right)}{\epsilon\left(\cos\theta_\mu, T_\mu, E_{avail}\right)_i \left(\Delta\cos\theta_\mu\right)_i \left(\Delta T_\mu\right)_i \left(\Delta E_{avail}\right)_i N_{\text{targets}}\, \Phi}$$

i truth space

j reco space

$N^{\text{sel}}\left(\cos\theta_\mu, T_\mu, E_{avail}\right)_j$	Number of selected events
$P\left(\cos\theta_\mu, T_\mu, E_{avail}\right)_j$	Purity of sample (estimated from simulation)
U_{ij}	Unfolding Matrix – to migrate from reco to truth space, using D'Agostini iterative unfolding
$\epsilon\left(\cos\theta_\mu, T_\mu, E_{avail}\right)_i$	Efficiency of sample (estimated from simulation)
$\left(\Delta\cos\theta_\mu\right)_i \left(\Delta T_\mu\right)_i \left(\Delta E_{avail}\right)_i$	Bin width of each variable

$\bar{\nu}_\mu$ CC-inclusive: Triple Differential Cross Section Measurement Strategy

$$\left(\frac{d^3\sigma}{d\cos\theta_\mu\, dT_\mu\, dE_{avail}}\right)_i = \frac{\sum_j U_{ij}\left(N^{\rm sel}\left(\cos\theta_\mu, T_\mu, E_{avail}\right)_j P\left(\cos\theta_\mu, T_\mu, E_{avail}\right)_j \right)}{\epsilon\left(\cos\theta_\mu, T_\mu, E_{avail}\right)_i \left(\Delta\cos\theta_\mu\right)_i \left(\Delta T_\mu\right)_i \left(\Delta E_{avail}\right)_i N_{\rm targets}\, \Phi}$$

i truth space

j reco space

$N^{\rm sel}\left(\cos\theta_\mu, T_\mu, E_{avail}\right)_j$	Number of selected events
$P\left(\cos\theta_\mu, T_\mu, E_{avail}\right)_j$	Purity of sample (estimated from simulation)
U_{ij}	Unfolding Matrix – to migrate from reco to truth space, using D'Agostini iterative unfolding
$\epsilon\left(\cos\theta_\mu, T_\mu, E_{avail}\right)_i$	Efficiency of sample (estimated from simulation)
$\left(\Delta\cos\theta_\mu\right)_i \left(\Delta T_\mu\right)_i \left(\Delta E_{avail}\right)_i$	Bin width of each variable
$N_{\rm targets}$	Number of nuclear targets in the detector

$\bar{\nu}_\mu$ CC-inclusive: Triple Differential Cross Section Measurement Strategy

$$\left(\frac{d^3\sigma}{d\cos\theta_\mu\, dT_\mu\, dE_{avail}}\right)_i = \frac{\sum_j U_{ij}\left(N^{\text{sel}}\left(\cos\theta_\mu, T_\mu, E_{avail}\right)_j P\left(\cos\theta_\mu, T_\mu, E_{avail}\right)_j \right)}{\epsilon\left(\cos\theta_\mu, T_\mu, E_{avail}\right)_i \left(\Delta\cos\theta_\mu\right)_i \left(\Delta T_\mu\right)_i \left(\Delta E_{avail}\right)_i N_{\text{targets}}\, \Phi}$$

i truth space
j reco space

$N^{\text{sel}}\left(\cos\theta_\mu, T_\mu, E_{avail}\right)_j$	Number of selected events
$P\left(\cos\theta_\mu, T_\mu, E_{avail}\right)_j$	Purity of sample (estimated from simulation)
U_{ij}	Unfolding Matrix – to migrate from reco to truth space, using D'Agostini iterative unfolding
$\epsilon\left(\cos\theta_\mu, T_\mu, E_{avail}\right)_i$	Efficiency of sample (estimated from simulation)
$\left(\Delta\cos\theta_\mu\right)_i \left(\Delta T_\mu\right)_i \left(\Delta E_{avail}\right)_i$	Bin width of each variable
N_{targets}	Number of nuclear targets in the detector
Φ	Beam flux

$\bar{\nu}_\mu$ CC-inclusive Data Results: $0 < E_{avail} < 100$ MeV

GENIE 3.0.6

- Results presented by E_{avail} bin, then in panels of varying angle
- The smallest E_{avail} bin (0 – 100 MeV) makes up 48% of the total sample
- Consists mainly QE and MEC events
- The **NOvA tune** shows good agreement with data since this region of E_{avail} phase space is MEC-enhanced
- **GENIE 'out-of-the-box'** underpredicts in all angle bins

QE	MEC	RES	DIS	Other
59.4%	35.4%	4.4%	0.6%	0.2%

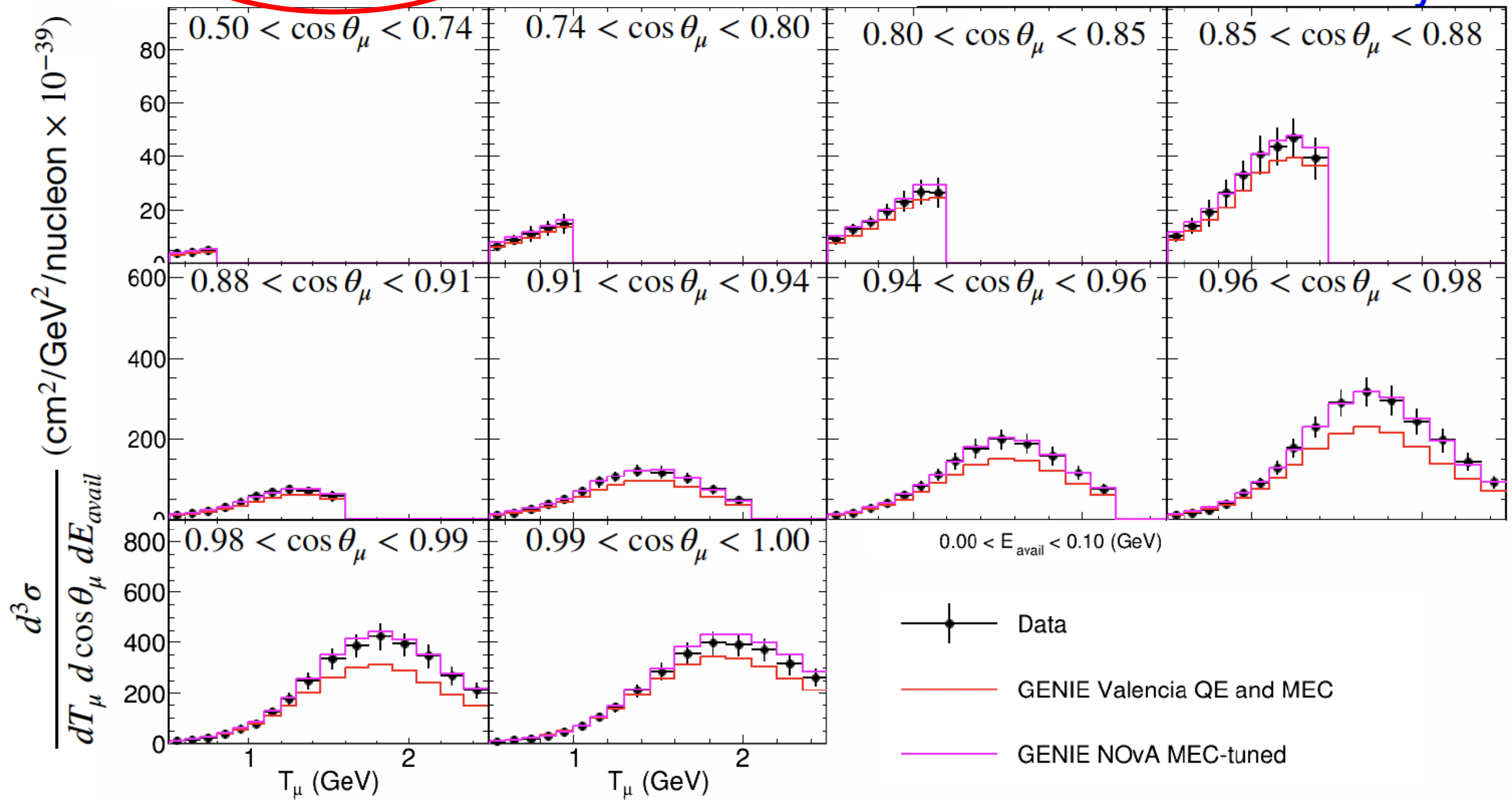

$\bar{\nu}_\mu$ CC-inclusive Data Results: $0 < E_{avail} < 100$ MeV

GENIE 3.0.6

QE	MEC	RES	DIS	Other
59.4%	35.4%	4.4%	0.6%	0.2%

- Comparisons can also be made with alternative neutrino event generators
- **NuWro** has a different shape – it uses a different QE interaction model (Llewellyn-Smith)
- **GiBUU** is the most consistent with NOvA data in this region of phase space – it is doing a good job of modelling QE and MEC interactions

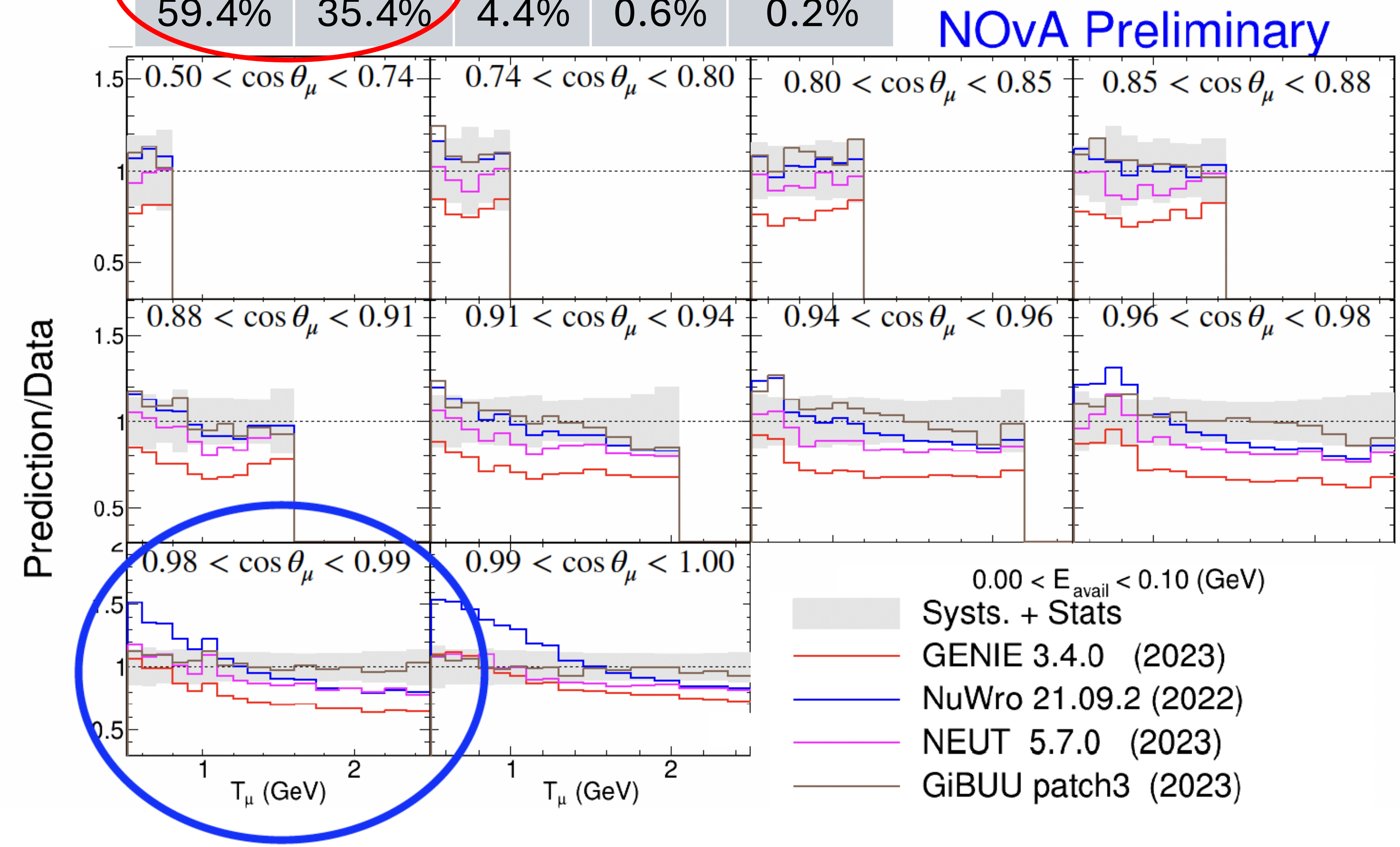

$\bar{\nu}_\mu$ CC-inclusive Data Results: 300 < E_{avail} < 600 MeV

GENIE 3.0.6

- The 300 – 600 MeV E_{avail} bin makes up 14% of the total sample
- Dominated by RES interactions
- Also rich in DIS events
- The **NOvA tune** and **GENIE 'out-of-the-box'** both overpredict data in this region of phase space

QE	MEC	RES	DIS	Other
3.9%	1.2%	68.0%	22.0%	4.9%

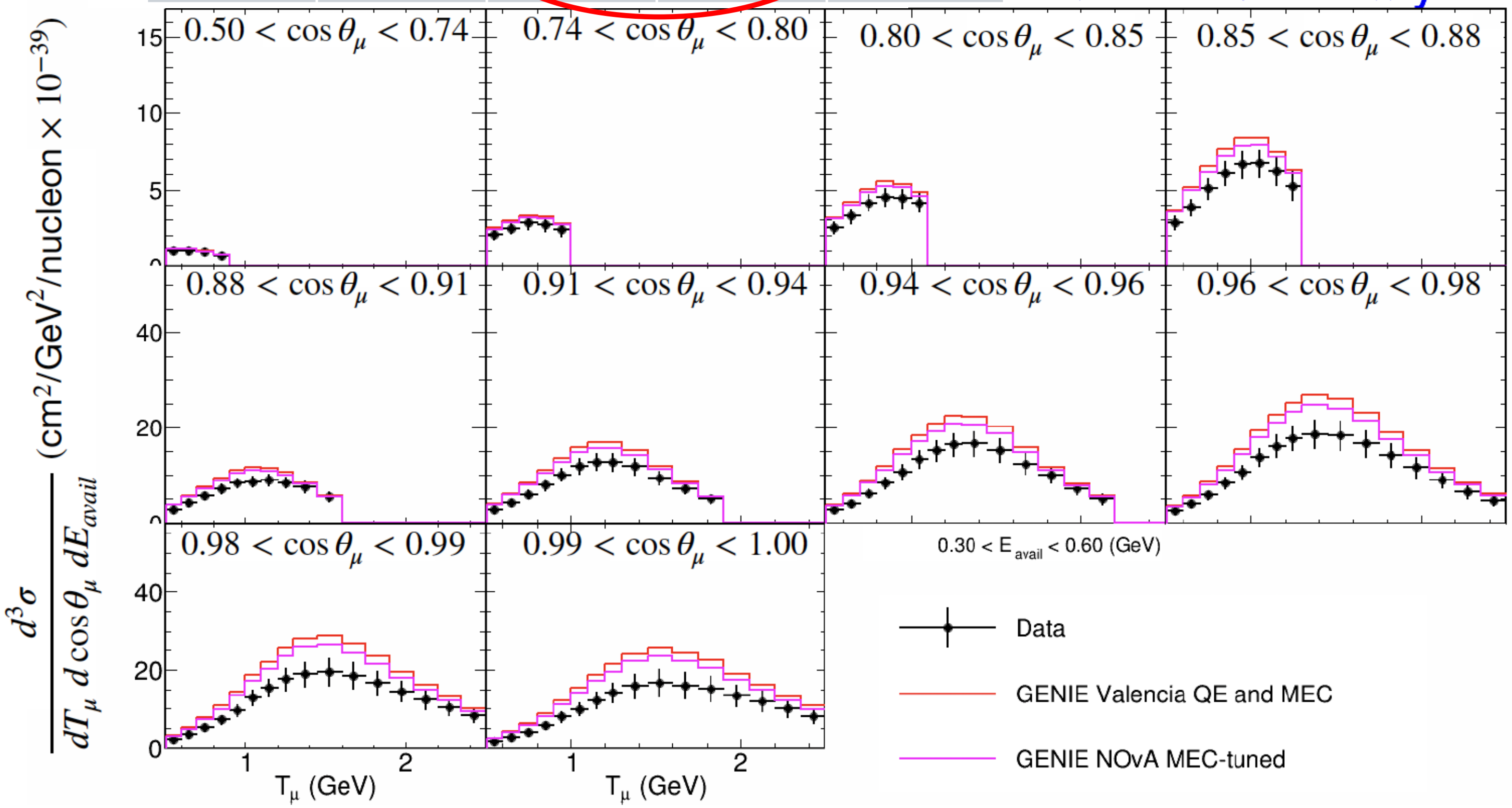

$\bar{\nu}_\mu$ CC-inclusive Data Results: 300 < E_{avail} < 600 MeV

GENIE 3.0.6

- In this region, generators all perform differently
- **NEUT** is the most consistent with data
- **GiBUU** mostly underpredicts compared with data

QE	MEC	RES	DIS	Other
3.9%	1.2%	68.0%	22.0%	4.9%

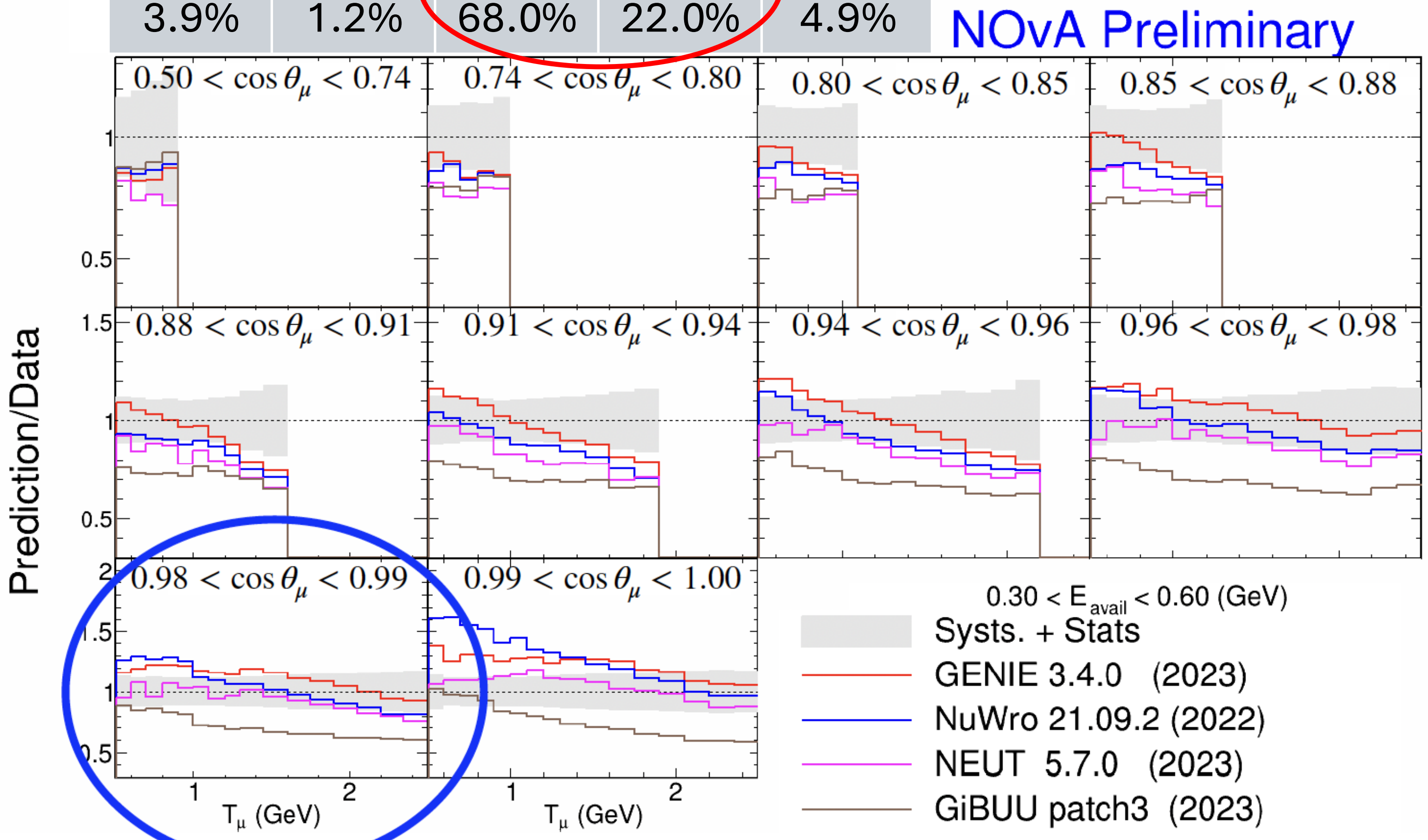

$\bar{\nu}_\mu$ CC-inclusive Data Results: E_ν and Q^2

GENIE 3.0.6

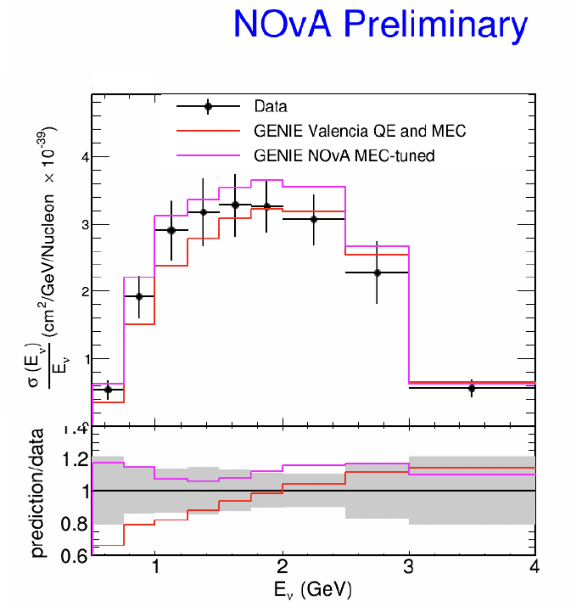

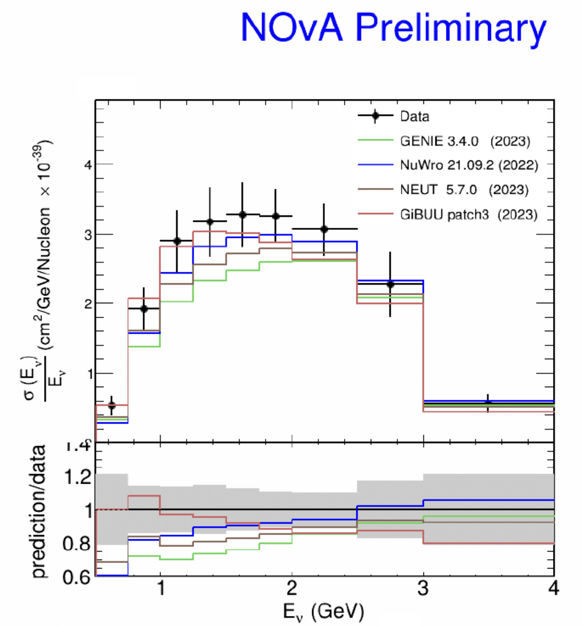

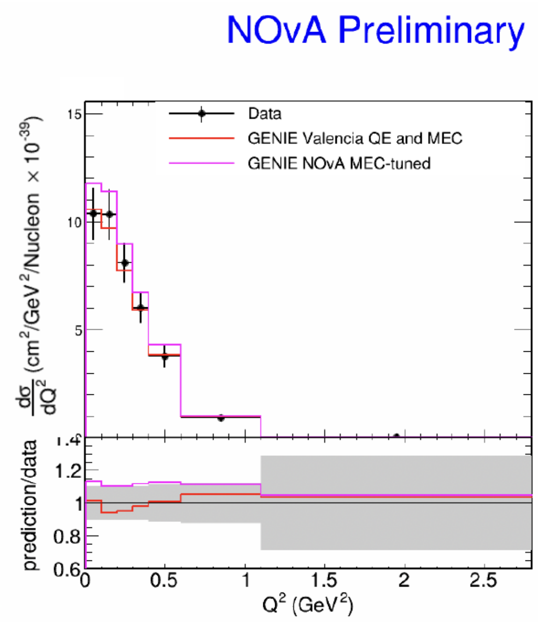

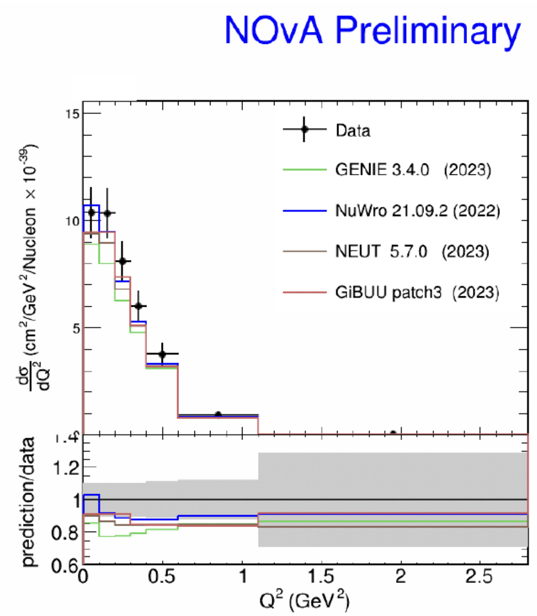

- **NOvA-tuned GENIE** slightly overpredicts data
- Except at the extremes in E_ν and at very low Q^2, all generators underpredict data
- Discrepancies lie mainly in the normalisation, but the shape is generally in agreement

ν_μ CC Low Hadronic Activity Analysis

arXiv:2410.10222

GENIE 2.12.2

- **Signal:** ν_μ CC interaction with interaction vertex in the fiducial volume of the ND, with $T_{proton} \leq$ 250 MeV, $T_\pi \leq$ 175 MeV

- **Selection:** ν_μ CC interaction with one reconstructed particle (the muon)
- **Aim:** to select a sample enhanced in QE and 2p2h, since RES and DIS are likely to produce at least two reconstructed particles

ν_μ CC Low Hadronic Activity Analysis

arXiv:2410.10222

GENIE 2.12.2

- **Signal:** ν_μ CC interaction with interaction vertex in the fiducial volume of the ND, with $T_{proton} \leq 250$ MeV, $T_\pi \leq 175$ MeV

- **Selection:** ν_μ CC interaction with one reconstructed particle (the muon)
- **Aim:** to select a sample enhanced in QE and 2p2h, since RES and DIS are likely to produce at least two reconstructed particles

- Analysis performed in T_μ, $\cos\theta_\mu$ and E_{avail} then integrated over E_{avail} to report a 2D differential cross section
- Also, 1D measurements of E_ν and Q^2

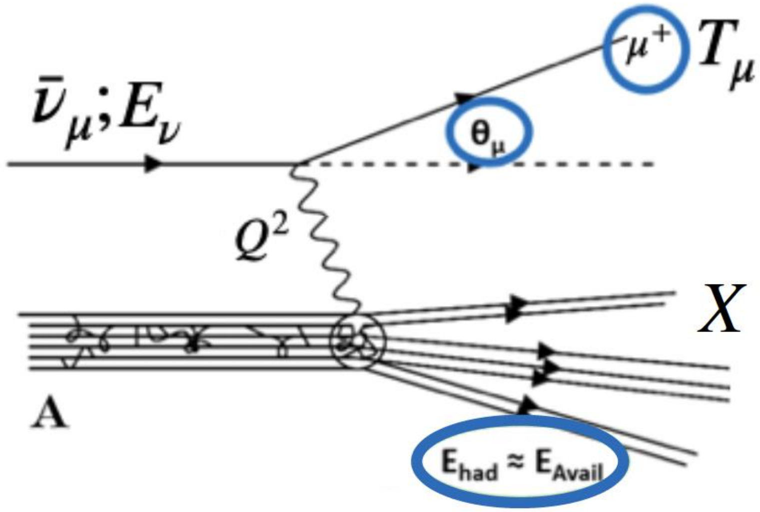

ν_μ CC Low Hadronic Activity Analysis

arXiv:2410.10222

GENIE 2.12.2

- Comparisons can be made to various 2p2h models
- **NOvA-tune** overestimates slightly in most bins, but still within error band
- **GiBUU** is the outlier, predicting a significantly higher cross section
- Other models (**empirical MEC**, **MINERvA-tuned MEC**, **Valencia model**, **SuSA-v2 model**) all predict a cross section lower than data

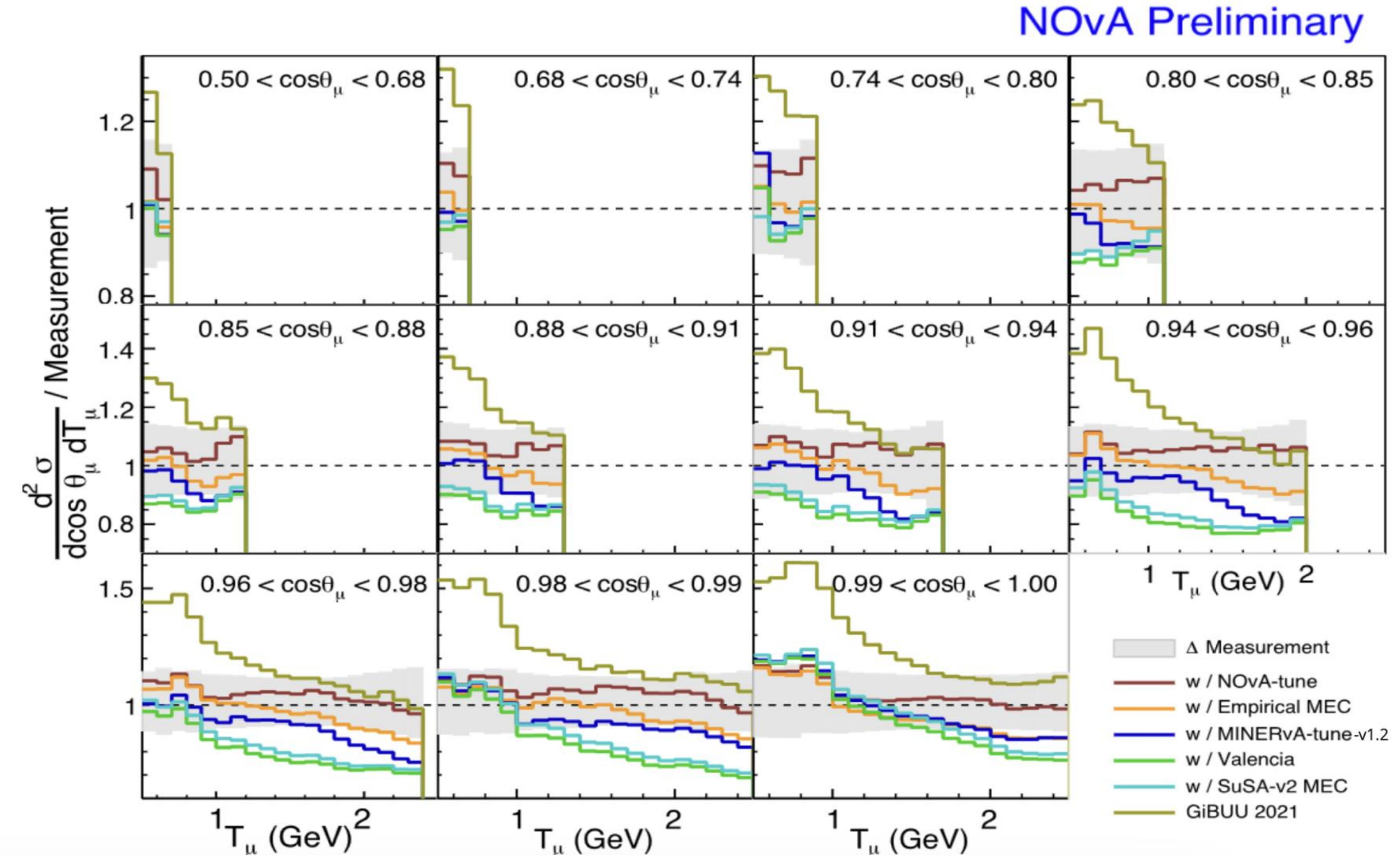

Double Differential Measurement of $|\vec{q}|$ and E_{avail}

arXiv:2410.05526

GENIE 2.12.2

- This analysis reports the 3-momentum transfer to the hadronic system, and E_{avail}, both as a double differential and as two 1D differential measurements
- Various 2p2h-MEC models are again compared to data
- The two theory-based models, **SuSAv2** and **Valencia**, greatly underpredict in the region of the rising slope of $d\sigma/d|\vec{q}|$ and at the cross section peaks

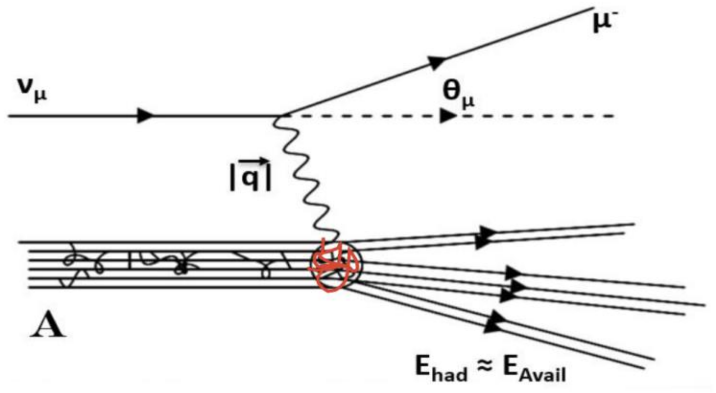

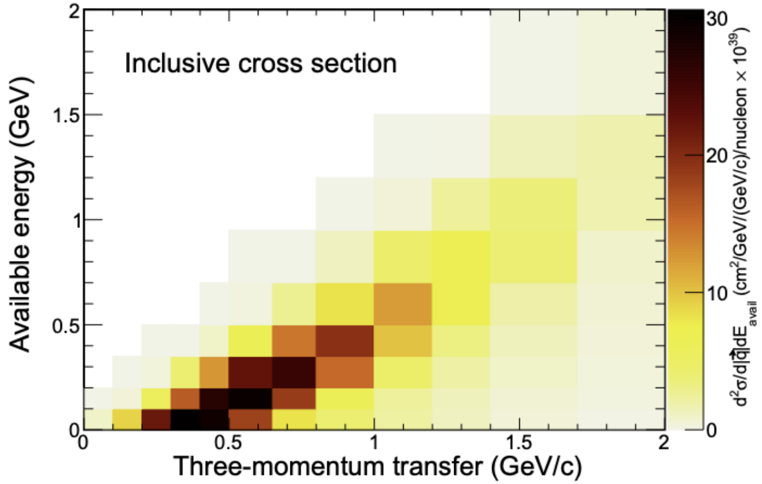

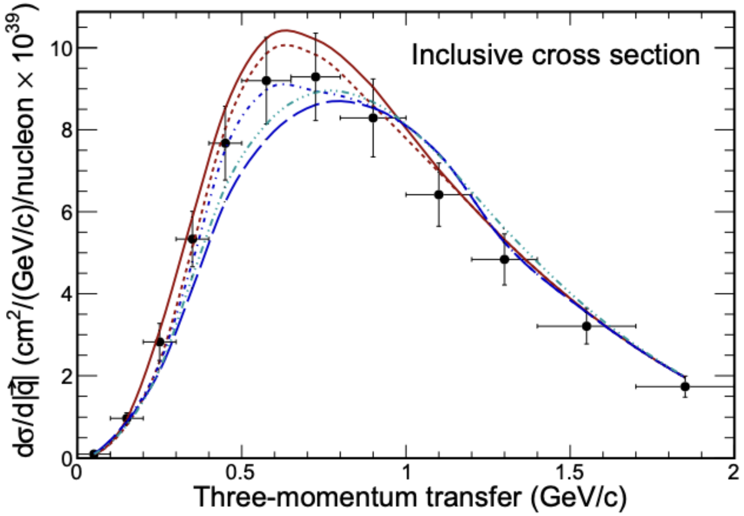

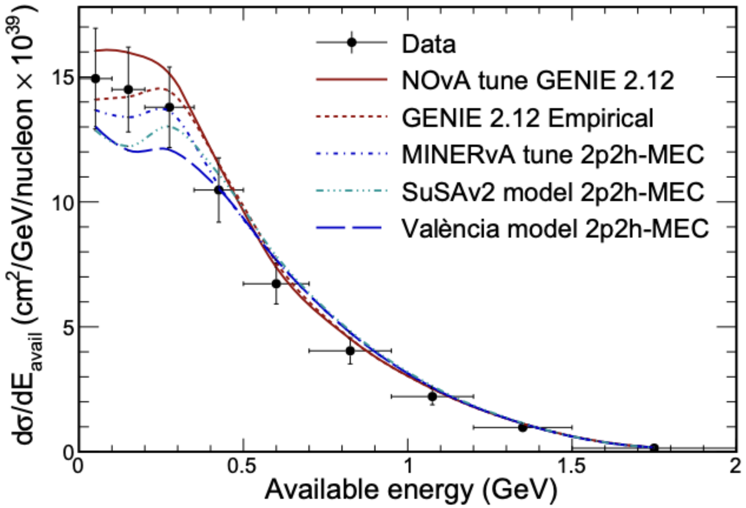

arXiv:2410.05526

2p2h Excess Cross Section

GENIE 2.12.2

- Templates of GENIE-based simulations of QE, RES, DIS and other interactions (mainly coherent scattering and inverse muon decay) are subtracted, to obtain a 2p2h excess cross section
- The two theory-based models are consistently below data, as is GENIE empirical MEC in most regions of $|\vec{q}|$, but the error bars are very large

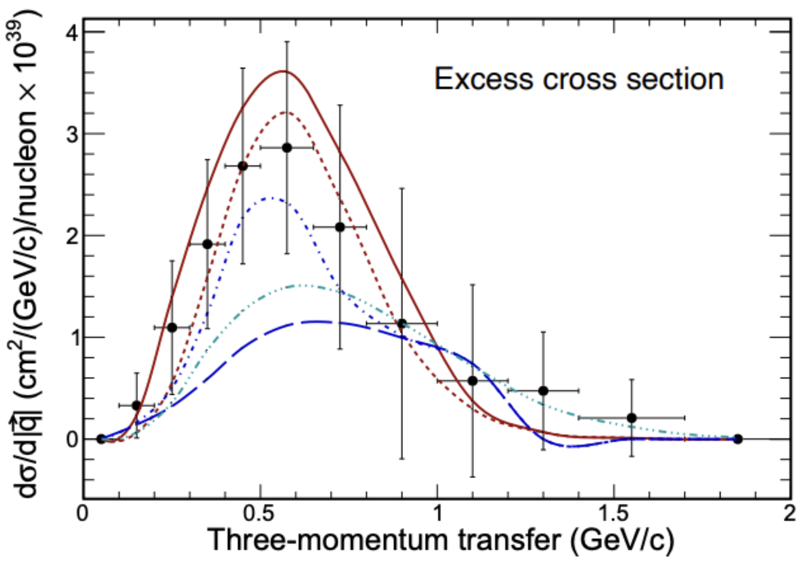

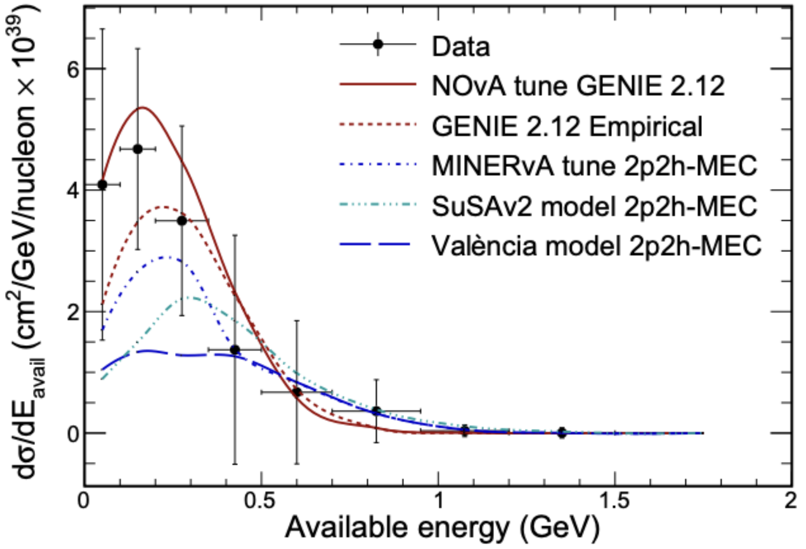

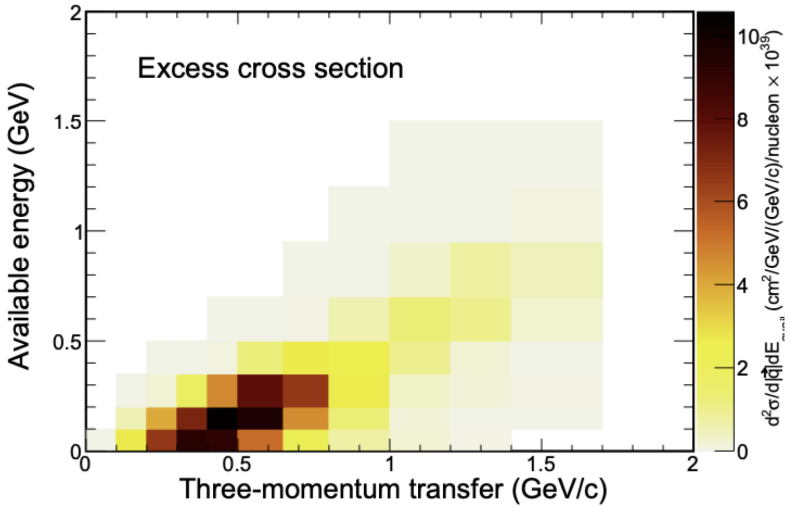

2p2h Excess Cross Section

GENIE 2.12.2

- Templates of GENIE-based simulations of QE, RES, DIS and other interactions (mainly coherent scattering and inverse muon decay) are subtracted, to obtain a 2p2h excess cross section

- The two theory-based models are consistently below data, as is GENIE empirical MEC in most regions of $|\vec{q}|$, but the error bars are very large

- The data-driven MINERvA and NOvA tunes match data more closely, which we can see from comparisons using χ^2 with covariances

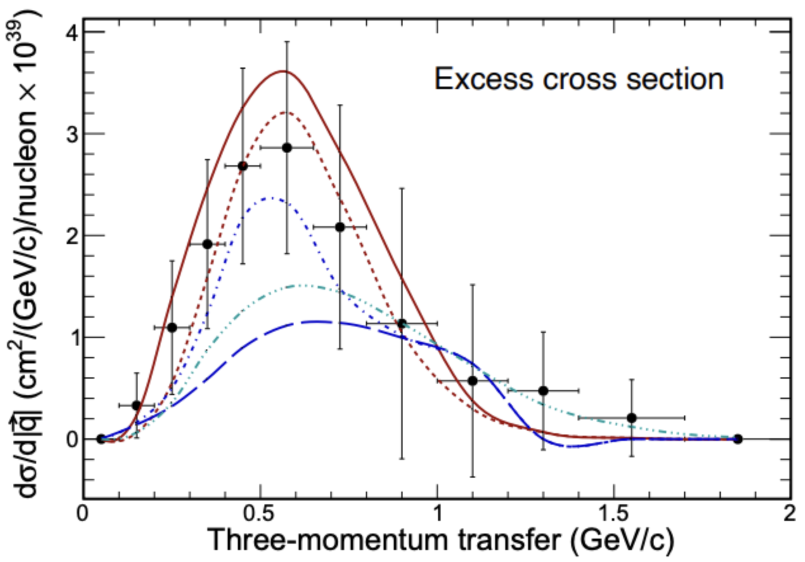

2p2h-MEC Model	χ^2	χ^2/DoF	Shape Only
NOvA tune 2p2h	103	4.69	3.90
GENIE Empirical	185	8.40	7.99
MINERvA tune 2p2h	84.4	3.83	4.11
SuSAv2 2p2h	177	8.04	9.15
València 2p2h	347	15.8	18.6

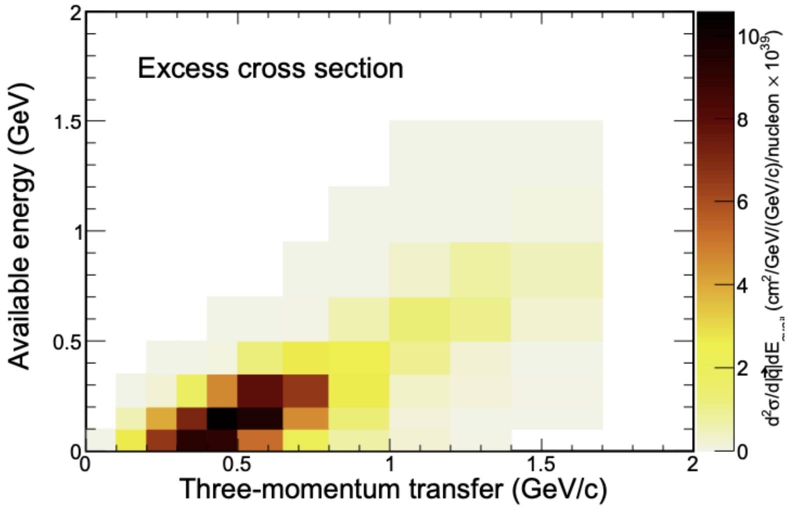

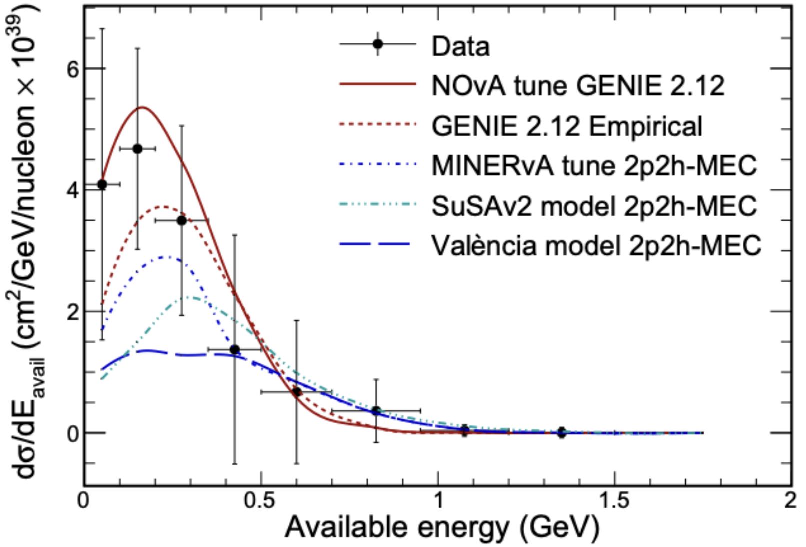

ν_μ CC-inclusive π^0 Production

PhysRevD.107.112008 (June 2023)

GENIE 2.10.2

- $\nu_\mu + A \rightarrow \mu^- + \pi^0 + X$
- A is the target nucleus, X represents all other final state particles, including other neutral or charged pions
- Detected mainly via the decay channel $\pi^0 \rightarrow \gamma\gamma$ (branching ratio of 98.8%)

- Measured total cross section, $(3.57 \pm 0.44) \times 10^{-39}\ \mathrm{cm}^2/\mathrm{nucleon}$, is 7.5% higher than the GENIE prediction, but within the range of uncertainties

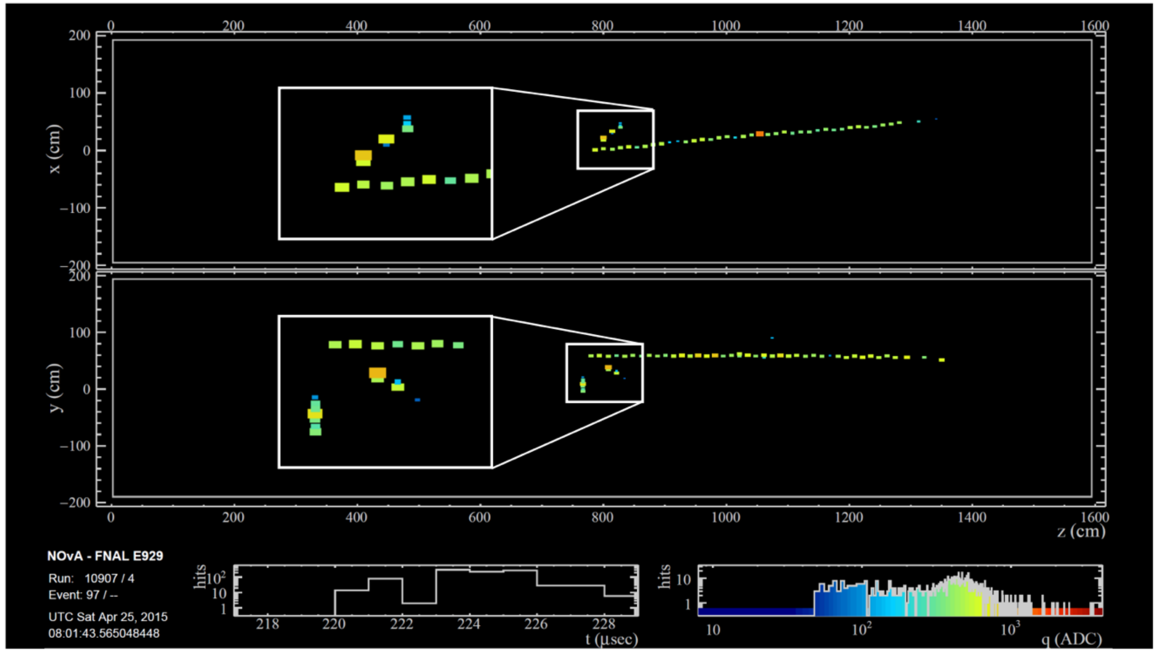

ν_μ CC-inclusive π^0 Production

PhysRevD.107.112008 (June 2023)

GENIE 2.10.2

- $\nu_\mu + A \rightarrow \mu^- + \pi^0 + X$
- A is the target nucleus, X represents all other final state particles, including other neutral or charged pions
- Detected mainly via the decay channel $\pi^0 \rightarrow \gamma\gamma$ (branching ratio of 98.8%)

- Measured total cross section, $(3.57 \pm 0.44) \times 10^{-39}\ \mathrm{cm}^2/\mathrm{nucleon}$, is 7.5% higher than the GENIE prediction, but within the range of uncertainties

- Reports differential cross sections in:
  - Neutral pion momentum, p_π, and scattering angle, $\cos\theta_\pi$
  - Muon momentum, p_μ, and scattering angle, $\cos\theta_\mu$
  - 4-momentum transfer, Q^2 and invariant hadronic mass, W

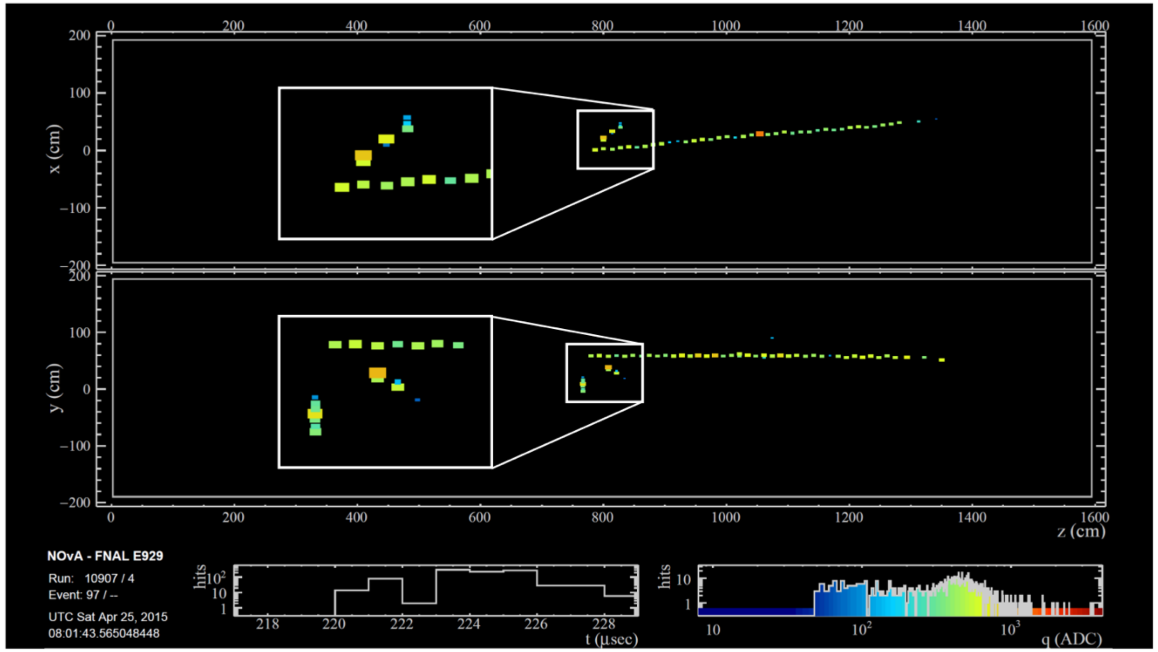

ν_μ CC-inclusive π^0 Results: Muon and Pion Kinematics

Muon kinematics cross sections separated by RES and DIS, and by pion multiplicity

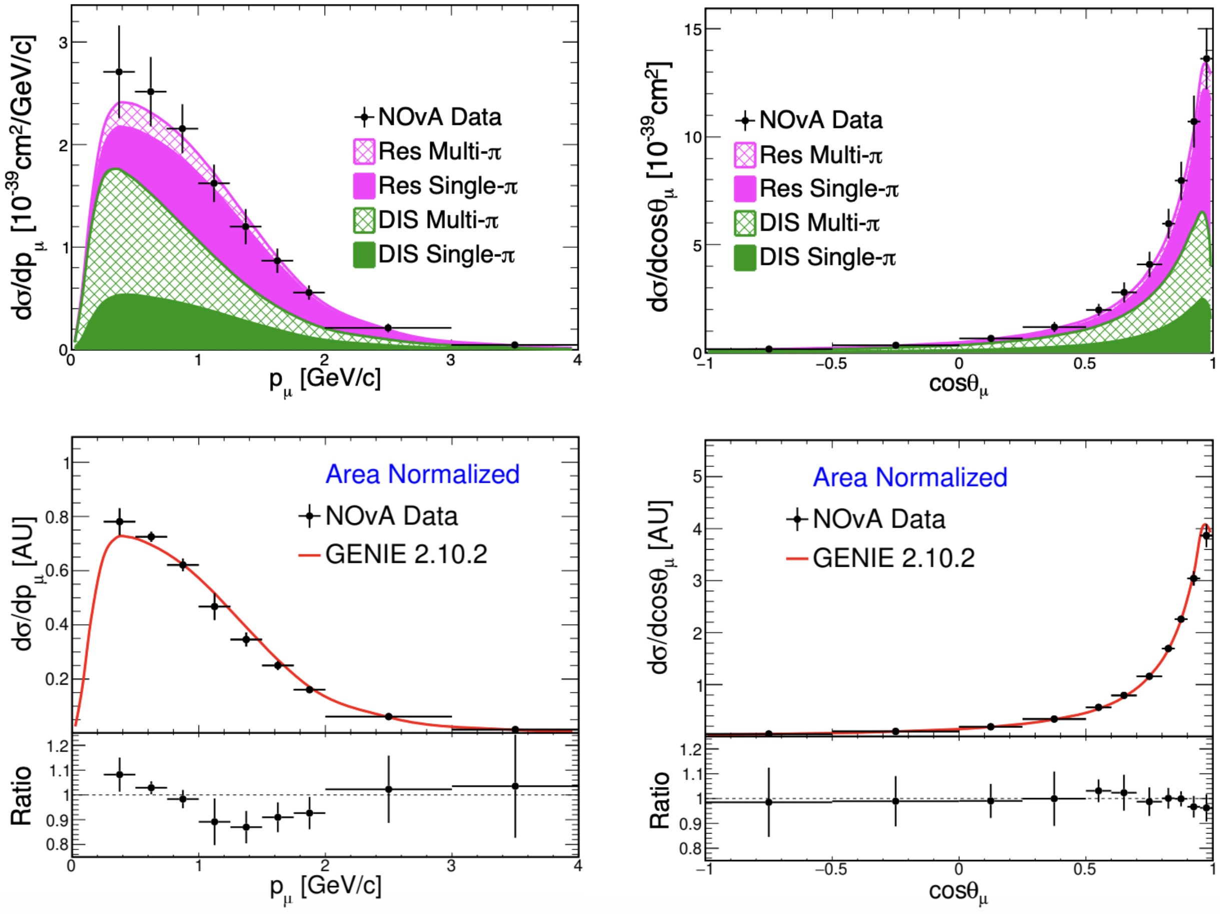

ν_μ CC-inclusive π^0 Results: Muon and Pion Kinematics

Muon kinematics cross sections separated by RES and DIS, and by pion multiplicity

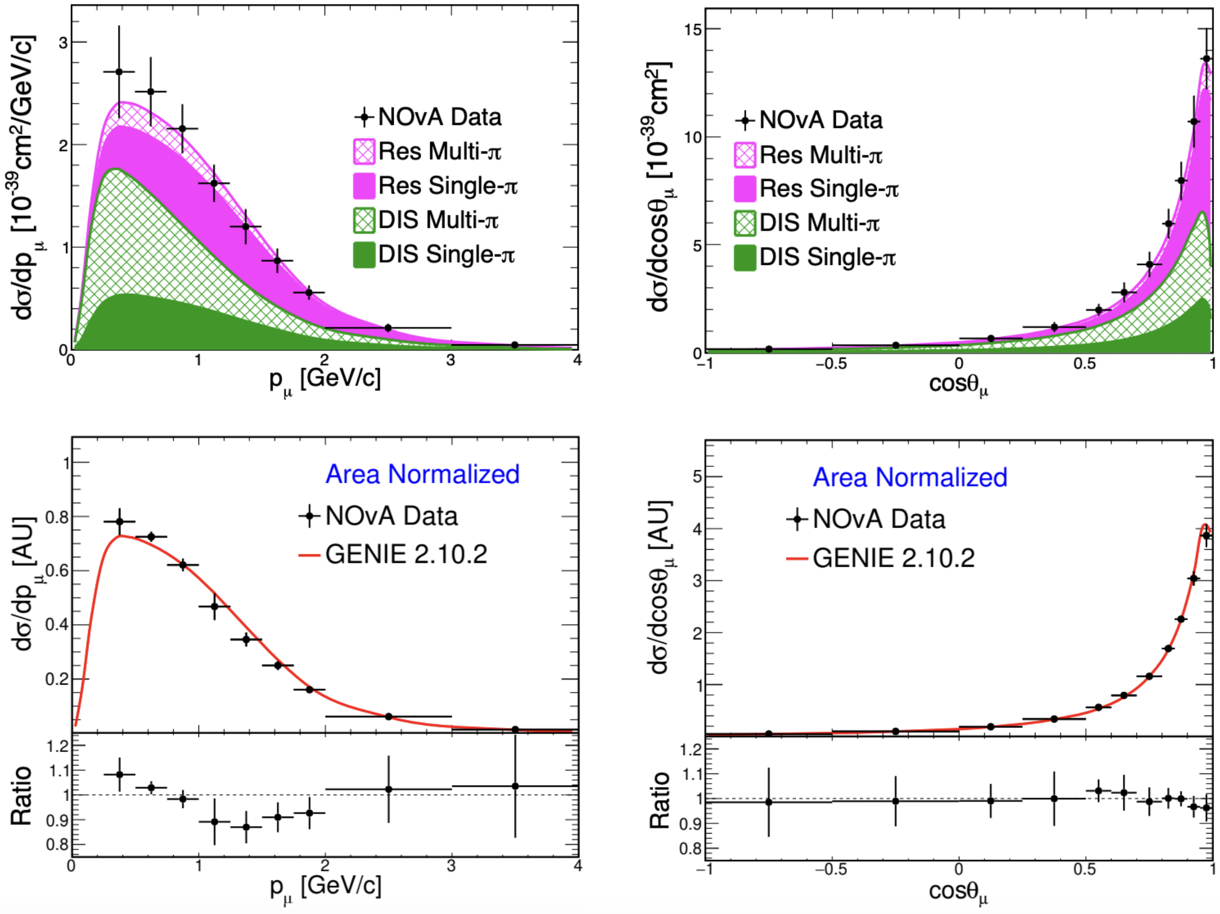

Pion kinematics cross sections separated by FSI channel. The $\pi + p \rightarrow \Delta_{1232}$ resonance is at around 0.3 GeV.

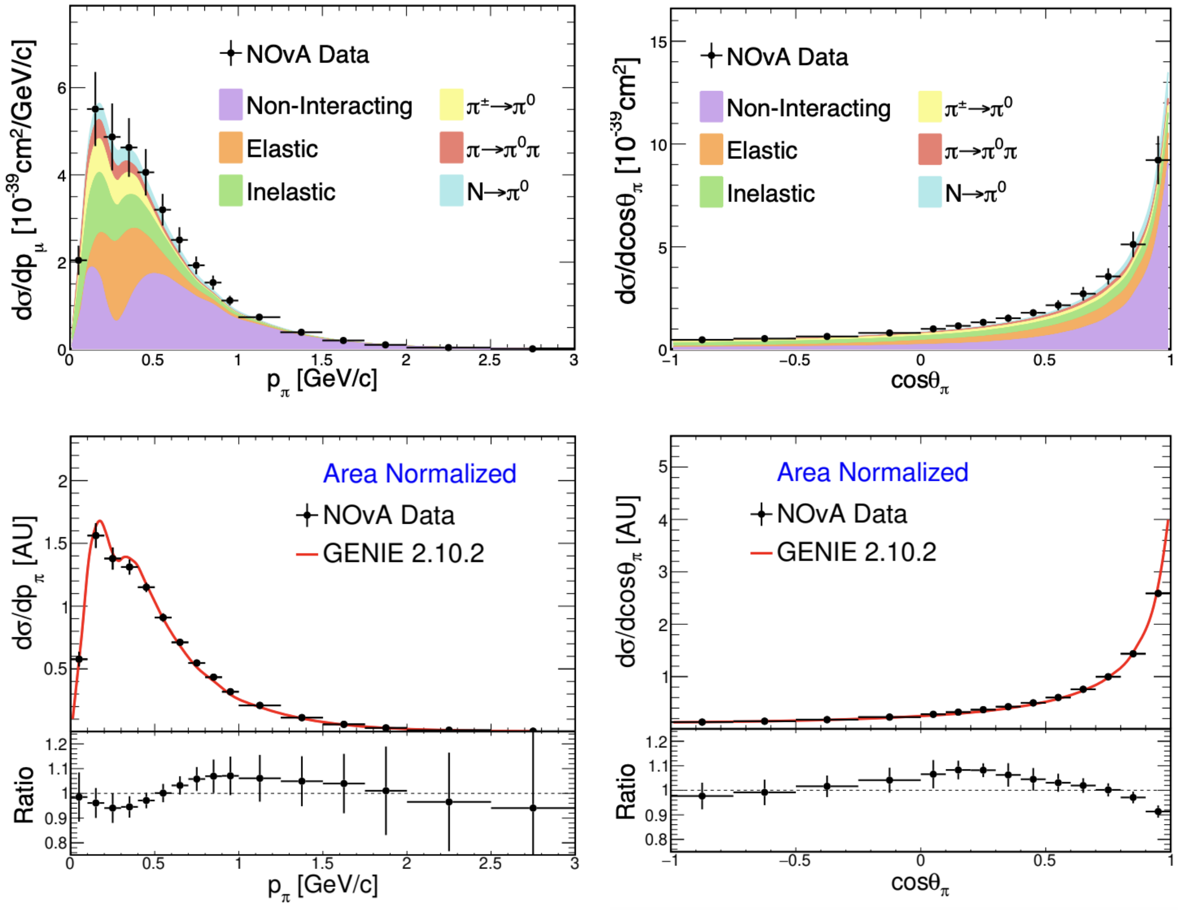

More NOvA Near Detector Results Coming Soon

- Many more cross section results are in the pipeline, including:
  - $\bar{\nu}_\mu$ CC π^0 measurement
  - $\bar{\nu}_e$ CC measurement
  - Both ν_μ and $\bar{\nu}_\mu$ CC 0-meson measurements
  - ν_μ charged pion measurements
  - $\bar{\nu}_\mu$ interactions on hydrogen
  - Measurement of the FHC ν-on-e flux

More NOvA Near Detector Results Coming Soon

- Many more cross section results are in the pipeline, including:
  - $\bar{\nu}_\mu$ CC π^0 measurement
  - $\bar{\nu}_e$ CC measurement
  - Both ν_μ and $\bar{\nu}_\mu$ CC 0-meson measurements
  - ν_μ charged pion measurements
  - $\bar{\nu}_\mu$ interactions on hydrogen
  - Measurement of the FHC ν-on-e flux

The newest Nova detector

A London-based lab(rador). Mostly detects food particles and sticks, but with 99.999% efficiency.

Thank you, on behalf of The NOvA Collaboration

Backup

ν_μ CC Low Hadronic Activity: E_{avail}

arXiv:2410.10222

GENIE 2.12.2

- Hadrons in the final state can influence purity, unfolding and efficiency, e.g.
  - if pions are misidentified as muons
  - If a hadronic shower hides the presence of a muon
  - If hadronic system is too close to detector edge and events fails containment cut

- This could introduce model dependences on the final-state hadronic system

- To try to reduce this, a 3D space including E_{avail} is used to apply purity, unfolding and efficiency corrections

$$\left(\frac{d^2\sigma}{d\cos\theta_\mu\, dT_\mu}\right)_i = \sum_{E_{avail}} \left(\frac{\sum_j U_{ij} \left(N^{sel}(\cos\theta_\mu, T_\mu, E_{avail})_j \, P(\cos\theta_\mu, T_\mu, E_{avail})_j \right)}{\epsilon(\cos\theta_\mu, T_\mu, E_{avail})_i \, (\Delta\cos\theta_\mu)_i (\Delta T_\mu)_i \, N_{\text{targets}} \, \Phi} \right)$$

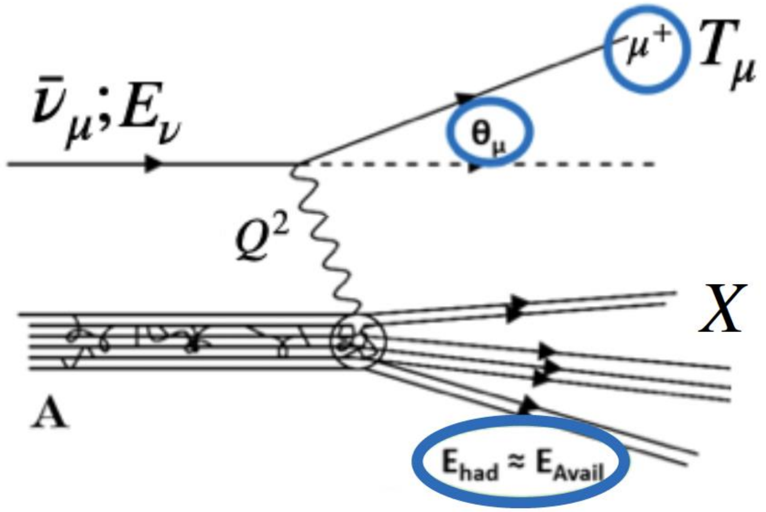

ν_μ CC-inclusive π^0 Results: W and Q^2

- Pion production cross sections separated into
    - RES: first resonance (Δ_{1232})
    - RES: all higher resonances
    - DIS
- Total cross section once again underpredicts the data
- But, when area-normalised we can see that the shape has good agreement

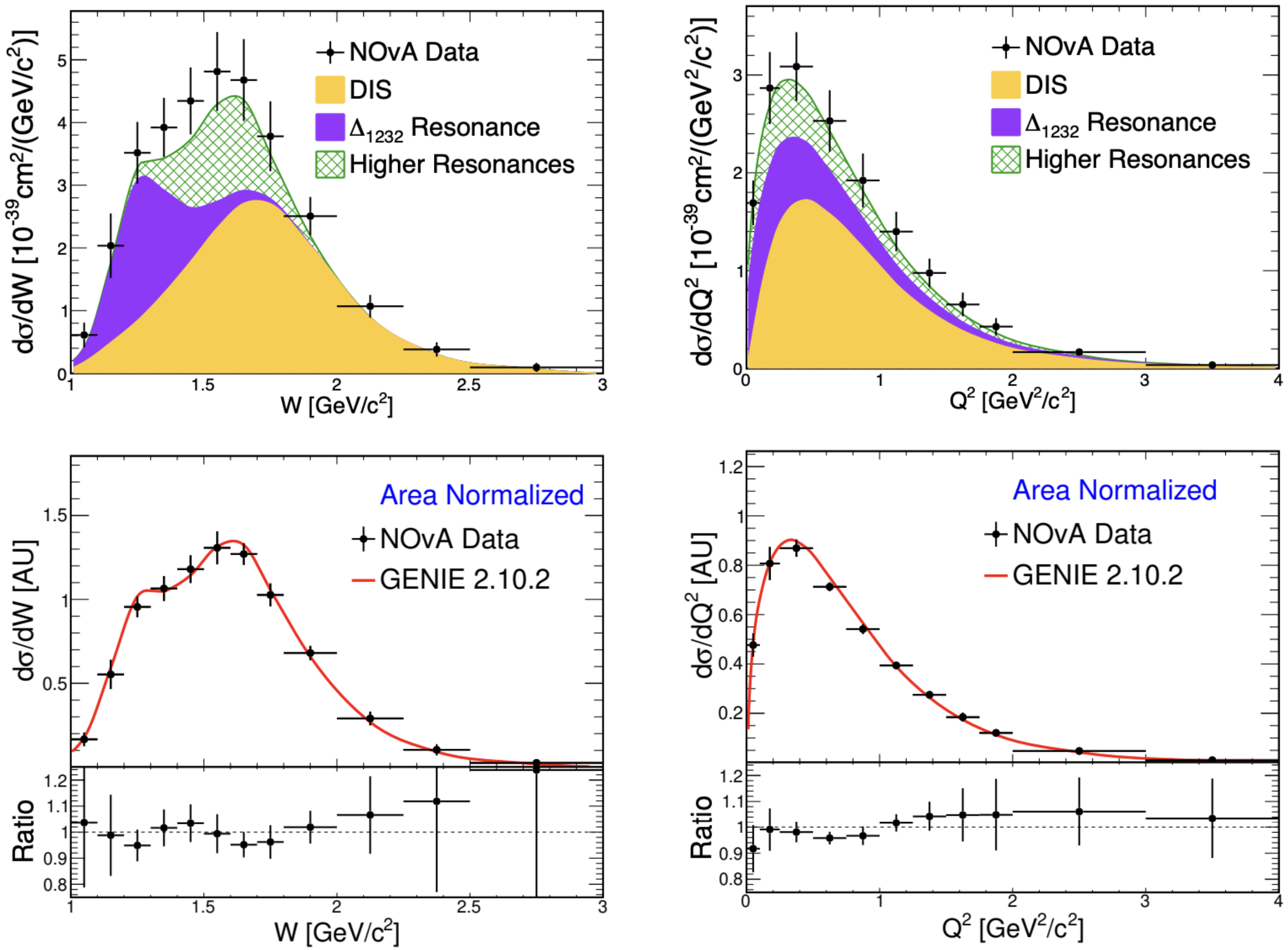

ν_μ CC-inclusive π⁰: Selection

PhysRevD.107.112008 (June 2023)

- $CC\pi^0$ID score is a log likelihood ratio representing the highest photon-like score among all tracks, apart from the muon track.

- Inputs are:
  - Bragg peak identifier – to measure the increase in dE/dx towards the end of the track
  - Average calorimetric energy of all hits within the track
  - Distance from the reconstructed event vertex to the start of the track
  - Largest number of consecutive planes with no deposited energy

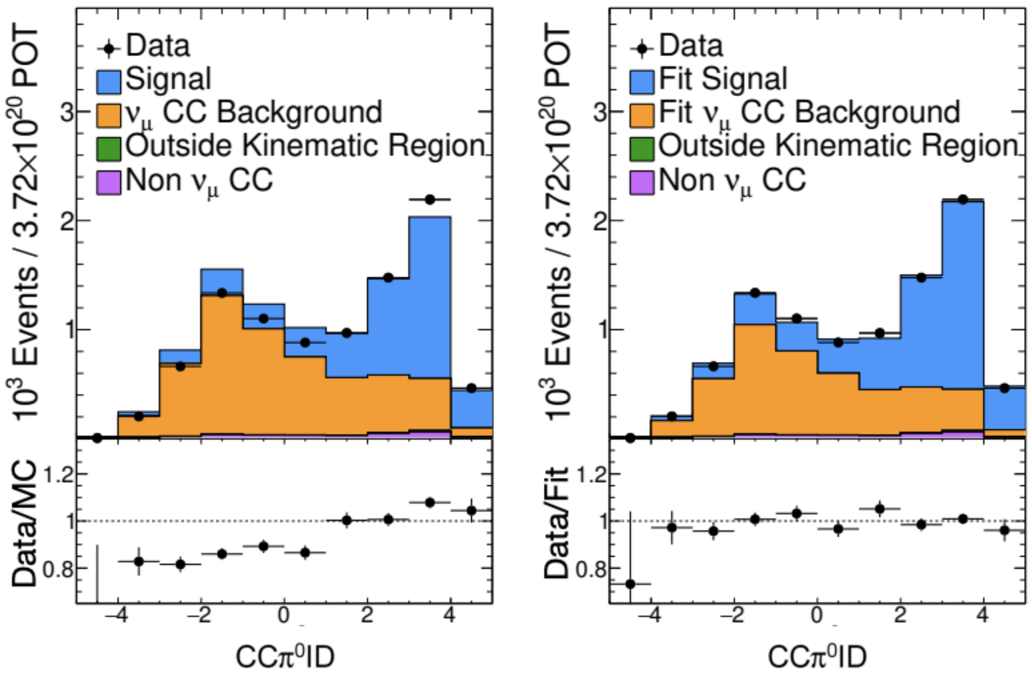

FIG. 7. An example fit to data in $CC\pi^0$ID for events reconstructed with $0.8 < p_\pi < 1.0\,\text{GeV}/c$. The left panel compares the unconstrained simulated $CC\pi^0$ID distribution and data while the right shows the simulation after constraining signal and background normalizations.